Nora virus proliferates in dividing intestinal stem cells and thereby sensitizes *Drosophila* flies to *Pseudomonas aeruginosa* intestinal infection and to oxidative stress

Adrien Franchet[1,4*], Samantha Haller[1*], Miriam Yamba[1], Vincent Barbier[1], Angelica Thomaz-Vieira[1,7], Vincent Leclerc[1], Stefanie Becker[3], Kwang-Zin Lee[1,5], Igor Orlov[2], Danièle Spehner[2], Laurent Daeffler[1,6], and Dominique Ferrandon[1†]

[*] These authors contributed equally to this work.

[1] UPR 9022 CNRS, IBMC, University of Strasbourg, France.

[2] UMR 7104 CNRS, U964 INSERM, IGBMC, University of Strasbourg, France.

[3] Institute for Parasitology and Research Center for Emerging Infections and Zoonoses, University of Veterinary Medicine Hannover, Hannover, Germany.

[4] Present address: Université Bourgogne Europe, Institut Agro, CNRS, INRAE, UMR CSGA, 21000 Dijon, France.

[5] Present address: Fraunhofer Institute for Molecular Biology and Applied Ecology (IME), Ohlebergsweg 12, Giessen, Germany.

[6] Present address: UMR 7178 CNRS, Institut Pluridisciplinaire Hubert Curien, Strasbourg, France.

[7] Present address: Institute of Translational Medicine and Liver Disease, Inserm U1110, Strasbourg, France.

† To whom correspondence may be addressed; e-mail: d.ferrandon@ibmc-cnrs.unistra.fr.

Abstract

The digestive tract represents the most complex interface of an organism with its biotope. Food may be contaminated by pathogens and toxicants while an abundant and complex microbiota thrives in the gut lumen. The organism must defend itself against potentially noxious biotic or abiotic stresses while preserving its microbiota, provided it plays a beneficial role. The presence of intestinal viruses adds another layer of complexity. Starting from a differential sensitivity of two lines from the same *Drosophila* wild-type strain to ingested *Pseudomonas aeruginosa*, we report here that the presence of Nora virus in the gut epithelium promotes the sensitivity to this bacterial pathogen as well as to an ingested oxidizing xenobiotic. The genotype, age, nature of the ingested food and, to a limited extent, the microbiota are relevant parameters that influence the effects of Nora virus on host fitness. Mechanistically, we detect the initial presence of the virus essentially in progenitor cells. Upon stress such as infection, exposure to xenobiotics, aging or feeding on a rich-food diet, the virus is then detected in enterocytes, which correlates with a disruption of the intestinal barrier function in aged flies. Finally, we show that the virus proliferates only when ISCs are induced to divide. We propose that enterocytes essentially get infected through lineage from progenitor cells and are not directly infected.

In conclusion, it is important to check that experimental strains are devoid of intestinal viruses when monitoring survival/life span of fly lines or when investigating the homeostasis of the intestinal epithelium as these viruses can constitute significant confounding factors.

Introduction

The digestive tract represents the most complex interface of the host with its environment as it involves a large surface, the presence of an important microbiota, the ingestion of food potentially contaminated by pathogens or toxicants, and the need for absorption of digested nutrients and solutes. Multiple concurrent infections or abiotic stresses are likely to be common, especially when the host feeds on decaying organic matter, as is the case for *Drosophila melanogaster*. Co-infection models with bacterial and viral pathogens in the gut are starting to be experimentally investigated and have revealed an enhanced susceptibility to combined infections that can be caused either by affecting pathogen transmission or by an inability to withstand tissue damage (Lian et al., 2022, and references therein).

Some twenty distinct viruses have been identified in wild Drosophila and around 30% of wild individuals are infected by at least one virus (Webster et al., 2015). A few of them are studied in the laboratory for the mechanisms of interaction with the host: *Drosophila melanogaster* Sigma Virus (DMelSV), Drosophila A virus (DAV), Drosophila C virus (DCV), Drosophila X virus (DXV), and Nora virus (Schneider and Imler, 2021; Webster et al., 2015). Nora is an enteric virus (Habayeb et al., 2006). Unlike other insect picorna-like viruses, its genome encodes four open reading frames corresponding to: a suppressor of RNA interference, VP1 (van Mierlo et al., 2012), replicative proteins coded by ORF2, the poorly characterized product of ORF3, and capsid proteins derived from ORF4 (Ekstrom et al., 2011). This virus infects common laboratory stocks where it appears to cause a persistent infection. It is transmitted horizontally and vertically via a fecal-oral route (Habayeb et al., 2009a; Habayeb et al., 2006). The Nora virus likely proliferates in the digestive tract, as large quantities of the virus are continuously released in the feces of infected flies. The virus does not appear to have major effects on host fitness, even though some damages to the intestinal epithelium have been reported (Habayeb et al., 2009a). However, the microbiota of flies infected by

69 Nora may change in quantity and bacterial diversity (Schissel et al., 2021). We then
70 wondered whether a persistent Nora virus infection could influence a secondary pathogenic
71 bacterial infection.
72 The *Drosophila* intestinal epithelium is simple, formed mostly by a monolayer of columnar
73 polyploid enterocytes (EC) and also comprises enteroendocrine cells and intestinal stem cells
74 (ISCs) and enterocytes progenitor called enteroblasts (Jiang and Edgar, 2011; Lemaitre and
75 Miguel-Aliaga, 2013). The microbiota is made up of few species, at most twenty, and is
76 usually dominated by two-three prevalent species such as *Acetobacter pomorum*,
77 *Lactobacillus plantarum*, or *Enterococcus faecalis,* but its composition changes with ageing
78 (Broderick and Lemaitre, 2012).
79 Immune defenses in the midgut include a chemical armamentarium, notably reactive oxygen
80 species (ROS) generated by the NADPH oxidase, NOX, and likely not Dual oxidase, and
81 antimicrobial peptides such as Diptericin (Ayyaz and Jasper, 2013; Buchon et al., 2013;
82 Ferrandon, 2013; Iatsenko et al., 2018; Jones et al., 2013; Kim and Lee, 2014; Liu et al., 2024;
83 Patel et al., 2019). Resilience, a complementary dimension of mucosal host defense also
84 known as disease tolerance (Medzhitov et al., 2012), is the ability of the intestinal epithelium
85 to maintain its homeostasis, for instance by a mechanism of cytoplasmic purge (Lee et al.,
86 2016) or the increased proliferation of ISCs that ultimately regenerate enterocytes damaged
87 either directly by pathogens or indirectly by the host's own immune response (Ferrandon,
88 2013, and references therein). ISC proliferation is regulated by the production of the growth
89 factor Unpaired 3 (Upd3) that activates the JAnus Kinase/Signal Transducers and Activators
90 of Transcription (JAK/STAT) pathway in ISCs (Buchon et al., 2009b; Herrera and Bach,
91 2019). Several models of gut infection have been developed in *Drosophila* (Bonfini et al.,
92 2016) and can be used to study coinfection with Nora virus. We have focused on *Serratia*
93 *marcescens* and *Pseudomonas aeruginosa* intestinal infections (Chen et al., 2025; Chen et al.,

2024; Cronin et al., 2009; Haller et al., 2018; Lee et al., 2016; Limmer et al., 2011; Nehme et al., 2007; Sina Rahme et al., 2022; Socha et al., 2023) and had not noticed major damages of *P. aeruginosa* oral infections on the integrity of the intestinal epithelium in contrast to another study (Apidianakis et al., 2009). *P. aeruginosa* bacteria are able to cross the intestinal barrier and to silently colonize inner tissues (Chen et al., 2024). They are initially found circulating in the hemolymph at low concentration. However, after a few days of continuous feeding on bacterial solution, the bacteria start proliferating in the hemolymph in a quorum-sensing-dependent manner and ultimately kill the host through bacteremia (Haller et al., 2018; Limmer et al., 2011).

Here, we demonstrate that Nora virus is a co-factor that synergizes with ingested bacteria or toxicants in *Drosophila* intestinal infection models, thus leading to an earlier demise of infected flies. We also report major effects of Nora infection on the lifespan of the flies under different feeding conditions. Mechanistically, we find that Nora virus initially infects ISCs and proliferates intensely upon ISCs divisions, ultimately leading to the contamination of enterocytes and gut barrier function disruption. Blocking the compensatory ISC proliferation by either inhibiting apoptosis in enterocytes or interfering with JAK-STAT signaling in ISCs protects flies from Nora pathogenesis through a drastic decrease of its load.

112 **Results**

113 **Nora virus-infected stocks are shorter-lived and more susceptible to some infections**

114 We noted that two Oregon-R (Ore-R) wild-type stocks kept by different investigators in the
115 laboratory, hereafter referred to as (SM) and (SC), displayed a remarkably distinct survival
116 pattern in one out of two models of intestinal infections (Limmer et al., 2011; Nehme et al.,
117 2007) in which flies respectively continuously feed either on *Pseudomonas aeruginosa* PA14
118 (Fig. 1A) or *Serratia marcescens* Db11 (Fig. S1A). Namely, the Ore-R (SM) was more
119 sensitive to PA14 and there was a slight trend toward higher susceptibility to Db11. We also
120 noted that Ore-R (SM) displayed a shorter lifespan under non-infected conditions either on
121 our standard food or on sucrose solution (Fig. 1B, Fig. S1B, and see below). We wondered
122 whether the difference might be due to an infection and checked the stocks for the presence
123 of common microbes known to affect *Drosophila* stocks (Haller et al., 2014; Lestradet et al.,
124 2014). The only notable difference we identified between the two stocks was the presence of
125 the Nora enteric virus in the infection-sensitive Ore-R(SM) (Fig. 1C).

126 We therefore examined the guts of flies from the two Ore-R stocks and did not detect any
127 major morphological differences. However, when we measured basal ISC proliferation by
128 counting phospho-histone H3-positive (PHH3) cells in the intestine, we found an enhanced
129 rate of ISC proliferation in the Nora-positive Ore-R(SM) stock (Fig. 1D). When we
130 challenged the Nora-negative Ore-R(SC) stock with *P. aeruginosa*, we found a small but
131 nevertheless significant increase in ISC proliferation. However, this *P. aeruginosa*-induced
132 increase was three-times larger in the Nora-positive Ore-R(SM) stock (Fig. 1D).

133 Overall, these observations suggest that flies infected with Nora have a lower fitness and are
134 more susceptible to infections than non-infected flies.

135

136 **Nora virus causes the enhanced susceptibility to *P. aeruginosa* intestinal infections**

137 As expected, bleaching the eggs laid by the Nora-infected Ore-R(SM) stock appeared to
138 eradicate the virus ((Habayeb et al., 2009b), Fig. 1E and Fig. S2A). This treatment did not
139 have a noticeable adverse impact as bleached stocks displayed a normal survival for at least
140 ten days on sucrose (Fig. S1E-I). Furthermore, cured Ore-R(SM) flies fed with *P. aeruginosa*
141 were less susceptible to this intestinal challenge than the uncured stock (Fig. 1F).
142 We placed our cured flies in a vial that had hosted infected males for several days for fecal-
143 oral transmission (Habayeb et al., 2009a) and found that they became again Nora-positive
144 over several generations (Fig. S2A). The reinfected stock was more sensitive to the ingestion
145 of *P. aeruginosa* than the cured stock (Fig. S2B). This correlated with an enhanced ISC
146 proliferation in the Nora virus reinfected flies, whether challenged with *P. aeruginosa* or not
147 (Fig. S2C).
148 The drawback of the fecal transmission route is that other enteric pathogens may be
149 transferred along with the Nora virus. To exclude this possibility, we used gradient
150 centrifugation to purify and concentrate Nora virus from an infected fly extract. This
151 preparation was homogenous with particles of the expected size when observed by cryo-
152 electron microscopy (Fig. 2A). Using RT-PCR, we confirmed the identity of the virus and
153 ruled out the presence of other *Drosophila* viruses (DAV, DCV, DBV, DTV, DXV, CrPV,
154 FHV…; see Table 1 Primer Sequence). Cured flies were fed on this pure viral preparation for
155 24 hours. This was sufficient to stably reinfect the stock over several generations (Fig. 2B).
156 As with the fecal contamination route, we observed that the flies reinfected with the pure
157 viral preparation were more sensitive to the ingestion of *P. aeruginosa* (Fig. 2C) and
158 displayed an enhanced rate of ISC proliferation in the gut (Fig. 2D). In terms of lifespan on
159 standard food or on sucrose solution, the re-infected stocks displayed a largely decreased
160 fitness (Fig. 2E-F), in contrast to the findings of (Habayeb et al., 2009a; Nigg et al., 2024)
161 who reported only a mild effect upon the injection of the Nora virus. Altogether, these results

162 demonstrate that Nora virus is responsible for the enhanced sensitivity to *P. aeruginosa*
163 intestinal infection.
164 We suspected that a polymorphism in the gene *pastrel* might be the cause of the different
165 susceptibility to Nora virus between Ore-R(SM) and Ore-R(SC) (Magwire et al., 2012). To
166 test this hypothesis, we determined by RT-PCR the presence of a *pastrel* sensitive or resistant
167 alleles (pst^S, pst^R) in several stocks commonly used in the laboratory. Strikingly, the sensitive
168 allele was found in homozygous condition only in the Ore-R(SM) stock, while it was
169 heterozygous in our *w* (A5001) stock (Fig. S1D). Interestingly, the *w* (A5001) (Thibault et al.,
170 2004) and the DD1 *cn bw* (Jung et al., 2001) stocks were found to be also harboring the Nora
171 virus, the latter one being pst^R/ pst^R (Fig. S1C-D). The *w* (A5001) and DD1 *cn bw* cured
172 stocks as well as the Canton-S stocks were all more susceptible to *P. aeruginosa* ingestion
173 after having been converted to a Nora-positive status by the prior ingestion of the purified
174 virus preparation (Fig. S1E-G). Since even stocks harboring two copies of the resistant
175 *pastrel* allele became more sensitive to ingested *P. aeruginosa* (Fig. S1D, S1F-G), we can
176 rule out that distinct *pastrel* alleles were also the cause of the enhanced sensitivity to bacterial
177 intestinal infections. Unexpectedly, the Ore-R(SC) strain appeared to be resistant to the
178 ingestion of Nora since it did not display an enhanced sensitivity to oral *P. aeruginosa*
179 infection (Fig.S1I). Thus, this line may harbor in addition to the homozygous pst^R allele a
180 polymorphism at an unidentified locus that restricts the Nora virus.
181 In the following, we will use the Ore-R(SM) cured stock as a Nora-negative control. We will
182 further characterize the impact of Nora virus on infected flies using the cured Ore-R(SM)
183 stock reinfected with the pure Nora preparation, which will be referred to as Nora-positive
184 flies.
185
186 **Nora virus is reducing host longevity largely independently of the microbiota**

187 We confirmed that Nora re-infected flies succumbed much earlier than Nora-negative control
188 flies when orally challenged with *P. aeruginosa* in a sucrose solution after five days of prior
189 feeding on our standard food or a rich food corresponding to our standard food containing
190 five times more yeast (Fig. S3A-B). Strikingly, we observed that an oral infection with PA14
191 increased the Nora burden (thrice on standard food and four-times on rich food). Actually,
192 both the Nora virus load and the *P. aeruginosa* titer was higher for flies fed on rich food (Fig.
193 3A, Fig. S3C). Of note, flies fed on rich food succumbed earlier to the challenge,
194 independently of their Nora status (compare S3B to S3A). We noted a correlation between
195 the Nora load in the absence or presence of PA14 and the measured proliferation of ISCs,
196 which held also on rich food (compare Fig. 3A and Fig. S3D).
197 As aging flies exhibit a dysbiosis that correlates with an impaired homeostasis of the
198 intestinal epithelium (Biteau et al., 2008; Buchon et al., 2009a; Choi et al., 2008), we also
199 compared the Nora burden in young (3-5 day-old) and old (30-35 day-old) flies and found an
200 about four-fold increase (Fig. 3B), which correlated with an enhanced rate of ISC
201 proliferation (Fig. S3E), in keeping with a previously published study (Hanson and Lemaitre,
202 2023). While checking for an increase of the microbiota load in old flies (Iatsenko et al.,
203 2018), we noted that the microbiota titer was much higher in Nora-positive than in Nora-
204 negative flies (Fig. 3C). This observation also held when flies were kept feeding only on a
205 sucrose solution (Fig. S3F). To determine whether the microbiota influenced the fitness of
206 Nora-negative or -positive flies, we first monitored their survival when kept on sucrose
207 solution. An antibiotic mix treatment substantially decreased the lifespan of Nora-negative
208 flies (Fig. S3G), possibly reflecting a positive impact of the microbiota on this amino-acid
209 depleted food solution even though the microbiota is minimal under these sucrose conditions
210 (Fig. S3F). In contrast, antibiotics treatment had no effect on Nora-positive flies feeding on
211 sucrose solution (Fig. S3G). Interestingly, the proliferation of ISCs was increased in

212 antibiotics-treated Nora-positive flies kept under these amino-acid depleted conditions (Fig.
213 S3H), which inversely correlates with the life span of those flies. We next monitored the
214 fitness of Nora-negative or -positive flies on our standard or on rich food. The antibiotic
215 treatment had a limited effect on Nora-negative flies with a somewhat enhanced fitness that
216 failed to reach statistical significance (Fig. 3D-E). In contrast, it significantly extended the
217 lifespan of Nora-positive flies on either standard or rich food (note that the detrimental effect
218 of the Nora virus is attenuated on rich food, at least for about two-thirds of their lives, until
219 they rapidly succumb). However, the antibiotics treatment failed by far to protect the flies to
220 the level of Nora-negative flies. We conclude that under these different feeding conditions,
221 the microbiota contributes at best only partially to the decreased fitness of Nora-positive flies.
222

223 **Nora virus contamination impairs the barrier function of the intestinal epithelium**

224 As an increased rate of ISC division may mirror a phenomenon of compensatory proliferation
225 driven by damage to enterocytes, we assessed the permeability of the gut of Nora-positive
226 flies, first using the SMURF assay on 30-day old flies; the SMURF assay monitors the
227 permeability of the gut barrier upon ingestion of a dye (Rera et al., 2011). The percentage of
228 SMURF-positive flies was much higher in 30-day old Nora-positive flies fed on rich food (a
229 time point corresponding to the death of 50% (LT50) of the flies in fitness experiments
230 shown in Fig. 3E) (Fig. 4A-B). In keeping with this result, when we plated hemolymph
231 collected from flies, we observed a strong microbial growth for that retrieved from SMURF-
232 positive flies, but not from SMURF-negative flies, whether Nora-positive or Nora-negative
233 (Fig. 4C). Thus, SMURF-positive flies do not only display an enhanced permeability to the
234 dye but also likely to the midgut microbiota, an indication of severe disruption of the barrier
235 function of the intestinal epithelium. These results were further confirmed after *P. aeruginosa*
236 ingestion: already after three days, the passage of PA14 through the intestinal epithelium was

237 much higher in Nora-positive than in Nora-negative flies (Fig. 4D). Of note, at Day 3, some
238 220 bacterial colonies on average were also retrieved from the hemolymph of Nora-positive
239 control flies that had not ingested PA14, possibly reflecting an early intestinal barrier
240 dysfunction in Nora-positive flies. Indeed, there was a detectable induction of a local immune
241 response in the midgut induced by PA14 ingestion only in Nora-positive flies at two days
242 instead of around five days for Nora-negative flies (Limmer et al., 2011), as monitored by
243 measuring *Diptericin* expression levels (Fig. 4E). This immune response is triggered by the
244 proliferation of *P. aeruginosa* in the hemolymph (Chen et al., 2024; Limmer et al., 2011).
245 We conclude that the Nora virus affects the integrity of the intestinal epithelium and its
246 barrier function.
247
248 **Nora does not directly influence the survival of flies to septic injury**
249 The experiments above show that the presence of the Nora virus in a stock increases its
250 susceptibility to ingested *P. aeruginosa.* Since *P. aeruginosa* ultimately causes a systemic
251 infection, we also tested whether Nora-positive flies would be more sensitive to other types
252 of systemic infections. As shown in Fig. S4A, we did not observe any difference in the
253 survival curves between Nora-positive or -negative flies exposed to spores of the
254 entomopathogenic fungus *Beauveria bassiana*, an infection model in which no macroscopic
255 wounds are inflicted. In contrast, Nora-positive flies succumbed significantly earlier than
256 Nora-negative control flies when challenged with the Gram-positive *Enterococcus faecalis* or
257 the Gram-negative *Enterobacter cloacae* bacterial pathogens in a septic injury model (Fig.
258 S4B-C). However, we found in control experiments that Nora-positive flies pricked with a
259 needle dipped into a sterile PBS solution succumbed at a rate that was similar to that
260 observed in flies submitted to a septic injury, whereas control Nora-negative flies were more
261 resistant to aseptic injury (compare Fig. S4D to Fig. S4B-C). Unexpectedly, *MyD88* flies

262 displayed an enhanced apparent sensitivity to a clean injury, a phenomenon we have
263 observed before and that depends on the endogenous microbiota of *MyD88* flies (Xu et al.,
264 2023). To understand why Nora-infected flies were more susceptible to a near-sterile wound,
265 we measured the proliferation rate of ISCs as it has been reported that injury triggers a ROS-
266 response, in the hypodermis, hemocytes, and in the gut that leads to enterocyte apoptosis and
267 an increased compensatory proliferation of ISCs (Chakrabarti and Visweswariah, 2020;
268 Takeishi et al., 2013). As reported, we observed a modest, statistically not significant,
269 increase of ISC proliferation in Nora-negative flies after injury of the cuticle (Fig. S4E).
270 Nora-positive flies displayed a higher basal rate of ISC proliferation that was however not
271 altered by injury, suggesting that gut damage is unlikely to account for the enhanced
272 sensitivity of Nora-positive flies to wounding of the cuticle. We finally compared the survival
273 rates of flies pricked with a clean needle to that of unchallenged controls and did not find any
274 significant difference (Fig. S4F). We conclude that the apparent sensitivity of Nora-positive
275 flies to clean injuries is actually due to the shortened lifespan of Nora-positive flies. This
276 effect only becomes apparent in systemic infections with mild pathogens that kill the flies
277 slowly (Fig. S4B-C).
278

279 **Nora virus is detected in intestinal stem cells in unchallenged flies and adopts an**
280 **enterocyte localization upon challenge**

281 Since the Nora virus is mostly detected in the gut by RT-qPCR (Habayeb et al., 2009a) and
282 plating assays (Ekstrom and Hultmark, 2016) (Fig. 5A) and since it affects the barrier
283 function of the intestinal epithelium, we raised an antibody against the virus, which is
284 essentially specific except for a cross reaction of the secondary antibodies with intestinal
285 muscles (compare Figs. 5B & S5A to 5C), which precludes drawing any conclusion as
286 regards a possible localization of the Nora virus also in these muscles, as has been previously

287 described for DCV oral infection (Ferreira et al., 2014). In contrast, a positive signal was
288 detected in basally located small triangular cells of the intestinal epithelium of flies that had
289 ingested the Nora virus five days earlier and not in non-infected controls (Figs. 5C-D, Fig. 5B
290 & Fig. S5A). The right panel of Fig. 5C displays a dividing stem cell that yields a basally
291 located ISC and a differentiating progenitor cell (enteroblast or enteroendocrine cell). Indeed,
292 a similar non-basally located small cell is shown in Fig. S5B. We confirmed the localization
293 of the Nora virus to progenitor cells of the intestinal epithelium by staining the Nora virus in
294 *esg-Gal4Gal80*^{ts} *>UAS-GFP* flies (Fig. 5D). The Nora-positive signal was always found in
295 the GFP-expressing progenitor cells. Using transgenic fly lines that express Dicer2-
296 fluorescent protein fusions (Donelick et al., 2020; Girardi et al., 2015), we noted that even
297 though the construct was expressed under the direct control of the poly-ubiquitin promoter
298 (*ubi-p63E*), we failed to detect the fusion protein in ISCs (Figs. 5E & S5C), even though GFP
299 is known to be stable in progenitor cells (Fig. 5D). If Dicer-2 were to be unstable specifically
300 in ISCs, this might account for the initial localization of the Nora virus to ISCs, a proposition
301 that would require further experimental confirmation.
302 We have shown above that young Nora-positive flies are more susceptible to *P. aeruginosa*
303 ingestion. We found that the Nora-positive flies were also more susceptible to the strongly
304 oxidizing agent paraquat in survival experiment (Fig. 5F). As for *P. aeruginosa* oral infection,
305 the ingestion of paraquat led to similarly enhanced levels of the viral load as monitored by
306 RTqPCR (Fig. 5G) and by staining with the Nora antibody (Figs. 5H & S5D).
307 Immunohistochemistry further revealed that the virus starts also proliferating within
308 enterocytes under pathogenic or chemical stress (Fig. 5H-I). Interestingly, aged flies raised on
309 our standard food or young flies raised on rich food also exhibited a growth of the virus in
310 enterocytes (Fig. S5E-I), in keeping with the increased viral burden found in these 30-day-old

311 flies (Fig. 3A-B). In addition, the detection of the Nora virus in enterocytes (Fig. 5I & Fig.
312 S5I) also correlated with an enhanced proliferation of ISCs (Figs. 3C & S3D).
313 In conclusion, the Nora virus is initially restricted to progenitor cells in basal conditions but
314 appears to start proliferating also inside enterocytes upon stress and/or increased proliferation
315 of ISCs. Importantly, Nora-positive cells were detected only in the posterior midgut (scheme
316 in Fig. S5J). These observations open the possibility that Nora virus is transmitted to
317 differentiating cells after ISC division (Figs. 5C & S5B) and then ultimately to enterocytes.
318

319 **ISC division promotes the proliferation of the Nora virus**

320 The above conclusion implies that ISC proliferation is likely needed to promote the
321 proliferation of the virus. To test this hypothesis, we used two complementary approaches
322 that rely on the fact that enterocyte damage triggers the compensatory proliferation of ISCs.
323 First, we measured the degree of apoptosis in epithelial cells through ApopTag/TUNEL
324 staining. We noted that Nora-positive bacteria do not display enhanced levels of apoptosis in
325 this tissue under basal conditions (Fig. 6A, Fig. S6A). However, the ingestion of *P.*
326 *aeruginosa* led to enhanced levels of apoptosis, significantly more so in Nora-positive flies
327 (Fig. 6A, Fig. S6B). In contrast, paraquat induced much higher levels of positive signals,
328 independently of the Nora status of the exposed flies (Fig. 6A, Fig. S6C). This situation was
329 roughly mirrored in the number of mitotic ISCs (Fig. 6B), although the degree of
330 proliferation induced by paraquat was similar to that induced by *P. aeruginosa* infection,
331 possibly mirroring an adverse effect of paraquat exposure to the division of ISCs (Chatterjee
332 and Ip, 2009).
333 Next, we attempted to block the induction of apoptosis in adult enterocytes by expressing
334 there the baculovirus p35 protein that inhibits executioner caspases (Hay et al., 1994). p35
335 did partially protect the flies from the noxious effects of *P. aeruginosa* ingestion, with a

336 relatively stronger effect on Nora-positive flies, which correlates with the higher number of
337 apoptotic cells measured in those flies (Fig. 6C-D, Fig. 6A). As expected, the expression of
338 p35 in enterocytes blocked the compensatory proliferation of ISCs (Fig. 6E). Strikingly, Nora
339 virus was obliterated in both control or *P. aeruginosa*-infected, originally Nora-positive, flies,
340 as monitored by RTqPCR (Fig. 6F) and by immunohistochemistry in 30-day old flies (Fig.
341 6G-H) for which less than ten Nora-positive progenitor cells per midgut were detected at best.
342 The second approach was to interfere with the signals that drive ISC proliferation upon
343 enterocyte damage. JAK-STAT pathway activation in ISCs promotes their division (Buchon
344 et al., 2009b; Cronin et al., 2009; Jiang et al., 2009). Silencing in ISCs the genes that encode
345 either the JAK-STAT pathway receptor Dome or the STAT92E transcription factor also
346 provided protection against ingested *P. aeruginosa*, in both Nora-positive and Nora-negative
347 cells (Fig. 7A-B). Indeed, the *upd3* gene encoding one Dome ligand and the gene encoding
348 the JAK-STAT-regulated inhibitor SOCS36E were induced in dissected midguts (crop and
349 Malpighian tubules not included) by *P. aeruginosa* ingestion, again more strongly so in Nora-
350 positive flies (Fig. 7C). This result was further corroborated using a transgenic fly line that
351 expresses an UPD3-GFP reporter protein (Fig. 7D). As expected, silencing *Dome* or *STAT*
352 abolished the compensatory proliferation of ISCs (Fig. 7E). Again, as for the ectopic
353 expression of p35 in enterocytes, blocking JAK-STAT pathway signaling in ISCs prevented
354 any proliferation of the Nora virus in midguts, whether infected orally with *P. aeruginosa* or
355 not (Fig. 7F). Microscopic analysis of immunostained posterior midguts confirmed that when
356 the JAK-STAT signaling pathway was blocked specifically in ISCs using a *Dome-Gal4*
357 driver line, Nora virus remained confined to progenitor cells and was not detected in
358 enterocytes (Fig. 7G-H).
359

360 **Discussion**

361 Nora virus infection is prevalent both in wild *D. melanogaster* flies and laboratory stocks
362 (Habayeb et al., 2006; Webster et al., 2015). It has originally been reported to have limited
363 effects on its host fitness, likely due to its proliferation that is mostly restricted to the
364 intestinal epithelium (Habayeb et al., 2009b). Here, in keeping with some more recent work
365 (Hanson and Lemaitre, 2023), we report that the presence of Nora virus may be a
366 confounding factor when performing intestinal infections or exposing flies to xenobiotics,
367 and more generally when investigating fitness in extended processes such as aging. Our data
368 support a model according to which Nora virus primarily infects intestinal epithelium
369 progenitor cells and largely remains latent/quiescent. However, exposure to a variety of
370 stresses that all lead to an increased proliferation of ISCs, apparently reactivates the virus and
371 results in the contamination of enterocytes. Ultimately, the generalized proliferation of Nora
372 within epithelial cells affects the barrier function of the midgut epithelium and leads to a
373 decreased fitness that leads to a premature demise of the infected flies (Fig. 8).

374

375 Our data document a low basal level of infection in young flies, which correlates with a
376 localization restricted to progenitor cells of the intestinal epithelium. Strikingly, a series of
377 parameters such as age, food nutritional value, pathogenic infection of the gut, and a strong
378 oxidizing agent all induce both an increased viral burden associated to the infection of
379 enterocytes, and proliferation of ISCs. Nora virus appears either to have relatively moderate
380 (Habayeb et al., 2009a; Hanson and Lemaitre, 2023; Nigg et al., 2024; Rogers et al., 2020;
381 Schissel et al., 2021) or intermediate to strong (this study; (Hanson and Lemaitre, 2023))
382 effects on host fitness. The finding that the higher nutrient quality of the food leads to
383 reduced effects on host fitness may partially account for these differences (Fig. 3D-E), even
384 though the Nora load was much higher on nutrient-rich food (Fig. 3A). The genetic

385 background may also contribute to these differences, even though we observed similar effects
386 of Nora infection on host fitness in a variety of strains fed on sucrose solution (Fig. S1 E-I). It
387 could also be that the strains used in other laboratories may have modifier genes in their
388 genetic background; indeed, one of Oregon strains we tested appeared to be nonpermissive
389 for Nora (Fig. S1I; see also (Hanson and Lemaitre, 2023)). Thus, the Nora load may differ in
390 the different laboratories and could account for the differences in host fitness(Hanson and
391 Lemaitre, 2023). Interestingly, the microbiota had opposite effects on host fitness depending
392 on the food source (positive on sucrose (Fig. S3G) *vs.* negative on standard or rich food (Fig.
393 3D-E)) (see also Arias-Rojas and Iatsenko, 2022 and references therein). We did observe a
394 higher microbiota titer in Nora-infected flies (Figs. 3C, S3F), which however did not
395 correlate with increased proliferation of ISCs at least on sucrose (Fig. S3H). Of note, strains
396 kept in our laboratory do not contain *Acetobacter* but mostly *Lactobacilli* strains in their
397 microbiota. Whether there is an increased diversity of the microbiota remains to be addressed.
398
399 Our results thus suggest that the virus is activated in dividing progenitor cells, especially
400 when the intestinal epithelium is stressed either by infection or exposure to xenobiotics, and
401 goes on proliferating in differentiated cells derived from these ISCs. The rate of ISC
402 proliferation is always higher in Nora-positive flies, suggesting that Nora contamination of
403 enterocytes may contribute in addition to stressors to their apoptosis and consequently lead to
404 an enhanced compensatory proliferation of ISCs. The finding that blocking apoptosis
405 enhances the fitness of Nora-positive flies to *P. aeruginosa* infection to the level of Nora-
406 negative flies while equally decreasing the proliferation of ISCs supports this proposition
407 (Fig. 6C-E). Hence, whenever ISC proliferation is triggered, the additional death of
408 enterocytes caused by Nora virus amplifies the phenomenon in a positive feedforward loop.
409 This model is further strengthened by the finding that the JAK-STAT ligand UPD3 is

410 expressed at a higher basal level and induced more strongly by *P. aeruginosa* infection in
411 Nora-positive flies than in Nora-negative flies. Thus, blocking either enterocyte apoptosis or
412 the regulatory pathway that drives compensatory ISC proliferation yields a similar protection
413 against the effects of Nora infection on fly fitness. More importantly, both experimental
414 manipulations lead to a spectacular decrease of the viral burden, even under *P. aeruginosa*
415 infection conditions (Fig. 6F & Fig. 7F).
416
417 We initially detect Nora-positive cells in basally located diploid progenitor cells. This
418 observation begs two questions. The first one is how basally located cells can become
419 infected and the second is why enterocytes that make up the apical part of the epithelium do
420 not get initially infected. The second question will be discussed further below. With respect
421 to the first one, we cannot formally exclude that enterocytes transport viral particles to the
422 basal side where they would then infect the progenitor cells. Indeed, many arboviruses cross
423 the intestinal barriers and transit through enterocytes in a polar manner (Hodgson et al., 2024).
424 Alternatively, progenitor cells are known to extend thin processes, some of which might
425 reach and probe luminal contents (Ohlstein and Spradling, 2006). These processes might
426 carry unidentified receptors for the Nora virus and enable the primary infection of progenitor
427 cells. In this view, it is an open possibility that enterocytes do not express these putative
428 receptors.
429
430 Our experiments point to an important role of initial replication of Nora virus in ISCs. With
431 the exception of hematopoietic stem cells that can be infected by retroviruses and herpes
432 viruses, mammalian germ cells, embryonic and adult stem cells have long been known to be
433 rather resistant to viral infections (Wu et al., 2019). Interestingly, mammalian stem cells do
434 not appear to rely primarily on interferon-based defenses, even though they do express a

435 subset of interferon-stimulated genes (ISGs) that contribute to the defense against viral
436 infections (Wu et al., 2018). Yet, they are not responsive to interferon, which is mediated
437 through JAK-STAT signaling, and instead rely to a large extent on RNA interference
438 (Maillard et al., 2013; Maillard et al., 2016; Poirier et al., 2021). Whereas interferon signaling
439 in mammals may have adverse effects on stem cell function because of antiproliferative
440 actions of some ISGs, JAK-STAT signaling in *Drosophila* ISCs promotes stem cell division
441 and is also involved in the subsequent differentiation of progenitor cells (Jiang et al., 2009).
442 Interestingly, picornaviruses and coxsackieviruses are known to productively infect activated
443 or proliferating cells while the infection of quiescent cells leads only to persistence or latency
444 (Feuer and Whitton, 2008). Future studies will tell at which step of the cell cycle the Nora
445 virus preferentially proliferates.
446
447 We have not addressed here whether the Nora virus is susceptible to host intestinal antiviral
448 defenses. A major antiviral defense in *Drosophila* is the RNAi pathway (Galiana-Arnoux et
449 al., 2006; van Rij et al., 2006), which however appears less active in the gut (Mondotte et al.,
450 2018), albeit oral DCV infection led to an increased viral load in *Ago2* but not *Dcr2* mutant
451 (Segrist et al., 2021). It will be interesting to determine whether the absence of a Dcr2-
452 fluorescent proteins fusions in progenitor cells that we report in this study rules out a role for
453 the RNAi pathway in intestinal host defense against the Nora virus. Nora virus-derived
454 siRNAs have been detected in fly tagmata, including the head (van Mierlo et al., 2012). In
455 addition, Nora VP1 protein has been shown to inhibit slicer activity of Ago2 (van Mierlo et
456 al., 2012). In contrast, it has been reported that Nora virus load is not altered in flies defective
457 for the RNAi antiviral pathway (Habayeb et al., 2009b), although the same study failed to see
458 an effect of the JAK-STAT pathway, which conflicts with our own results (this study). It
459 should be emphasized that this study was performed on young 3-5day old flies in which Nora

460 virus is detected only in progenitor cells and not in enterocytes. Thus, it is an open possibility
461 that the RNAi machinery is efficient in preventing the primary infection of enterocytes (but
462 would not impair polarized transit to the basal side of enterocytes). Consequently, only
463 enterocytes derived from infected progenitor cells would allow the contamination of
464 enterocytes. Possibly, a high load of the virus in progenitor cells would allow it to interfere
465 with the RNAi machinery in developing enterocytes. The PVR/ERK pathway has been
466 documented to play a role in enterocyte host defense against viral infections (Sansone et al.,
467 2015). However, it needs to be primed by the microbiota through the PGRP-LC/IMD
468 pathway and Pvf2 induction in enterocytes. Given the opposite effects of the microbiota on
469 Nora-infected fly fitness depending on the food source, it appears unlikely that the PVR/ERK
470 signaling pathway plays an essential role in host defense against the Nora virus. In addition,
471 the likely absence of *Acetobacter* species in the microbiota of our fly strains on our food
472 likely limits the induction of Pvf2 expression in enterocytes via the IMD pathway since
473 *Lactobacilli* do not induce it (Sansone et al., 2015). The STING/Relish pathway is another
474 important systemic antiviral pathway (Ai et al., 2024; Cai et al., 2020; Goto et al., 2020;
475 Segrist et al., 2024), which is also relevant to that of the intestinal epithelium. However,
476 current data suggest it is mostly active in enterocytes (Nigg et al., 2024; Segrist et al., 2021).
477 Importantly, in the case of DAV, another prevalent intestinal virus, it is the EGFR pathway in
478 enterocytes and not the JAK-STAT pathway acting in progenitor cells that is important for
479 DAV proliferation. In addition, DAV is mostly found in enterocytes and only occasionally in
480 progenitor cells (Nigg et al., 2024). Thus, while this axis of defense may not be essential once
481 stem cells are proliferating, it might protect the enterocytes in the primary fecal infection.
482 As emphasized by other investigators, intestinal viruses may be confounding factors of
483 studies on aging and intestinal physiology, especially as regards the proliferation of ISCs
484 (Hanson and Lemaitre, 2023; Nigg et al., 2024). Our results further add intestinal bacterial

infections and exposure to toxicants to this list and more generally any study in which the process under investigation involves monitoring the survival of flies for periods of time over eight days. Finally, we have attempted to establish a Nora-free facility and bleached some 100 fly lines that tested Nora-negative on whole fly extracts. However, after a few months many of these lines tested positive for Nora. It is an open possibility that some fly strains cannot be cured (we had to go through several rounds of bleaching to cure from Nora contamination our Ore-R (SM) stock). Alternatively, a more sensitive test for Nora detection should be used, starting on dissected guts and for instance digital PCR (see also (Nigg et al., 2022)).

495 **Materials & Methods**

496 **Drosophila stock and husbandry**

497 Wild-type Ore-R(SM) Nora(+) and Ore-R(SC) Nora(-) fly stocks were found in our
498 laboratory. Both stocks of wild-type *Oregon-R* flies tested negative for *Wolbachia* infection.
499 Stock used for the septic injury and natural infections are the following: wild-type w^{A5001}
500 (Thibault et al., 2004), mutant *MyD88c03881* (Tauszig-Delamasure et al., 2002), mutant DD1
501 *cn bw* (Rutschmann et al., 2000), key^{cO2831} (Ferrandon D., unpublished), *NP1-Gal4* (Cronin et
502 al., 2009), *esg-Gal4Gal80*^{ts} (Micchelli and Perrimon, 2006), *delta-Gal4* (Zeng et al., 2010),
503 VDRC GD control line (#6000 VDRC), *UAS-dome*^{RNAi} (#36355 GD VDRC) (Borensztejn et
504 al., 2013), Bloomington control line *UAS-mCherry*^{RNAi} (#35787 Bloomington Drosophila
505 Stock Center) (Borensztejn et al., 2013), *UAS-p35* (#5073 Bloomington Drosophila Stock
506 Center) (Hay et al., 1994; Rahmatika et al., 2019), *UAS-Stat92E*^{RNAi} (#26899 Bloomington
507 Drosophila Stock Center) (Nagai et al., 2023), and *upd3::GFP* (Zhou et al., 2013).

508

509 All stocks have been checked for the presence of known pathogens and symbiont besides
510 Nora virus (Haller et al., 2014; Lestradet et al., 2014; Niehus et al., 2012). Fly stocks were
511 kept at 25°C and nearly 60% humidity, on a standard semi-solid cormeal medium (6.4% (w/v)
512 cornmeal (Moulin des moines, France), 4.8% (w/v) granulated sugar (Erstein, France), 1.2%
513 (w/v) yeast brewer's dry powder (VWR, Belgium), 0.5% (w/v) agar (Sobigel, France), 0.004%
514 (w/v) 4-hydroxybenzoate sodium salt (Merck, Germany)). For lifespan analysis, 3 x 20
515 female flies were kept at 25°C with 60% humidity, on standard fly food. Flies were
516 transferred without anesthesia on fresh food every 4 days. For survival test on a sucrose only
517 diet, 3x 20 female flies were fed on 2 mL on a 50 mM sucrose solution and kept at 25°C with
518 60% humidity.

519

520 **Microbial strains, growth conditions and infection**

521 Microbes were grown in these conditions: *Pseudomonas aeruginosa* PA14 in Brain-Heart-
522 Infusion Broth (BHB), overnight, at 37°C (Rahme et al., 1995); *Serratia marcescens* Db11
523 (Nehme et al., 2007) in Luria Bertoni Broth (LB), overnight, at 37°C; *Enterobacter cloacae*
524 (Lemaitre et al., 1997), in LB, overnight, at 30°C; *Enterococcus faecalis* (TX0016) in BHB
525 overnight, at 37°C; *Beauvaria bassiana* (Lemaitre et al., 1997) on malt agar plates at 25°C.
526 Intestinal infections were performed as described previously with PA14 (Haller et al., 2014)
527 and Db11 (Lee et al., 2016). Briefly, flies were continuously feeding on a sucrose solution
528 containing the bacteria at the indicated OD and deposited on filter pads in the absence of
529 standard food. In the case of *S. marcescens* 100 µL of 100 mM sucrose solution was added to
530 the cage every day. Infected and control flies were kept at 25°C. For PA14 infection, 3x 20
531 female flies were used per experiment. For *E. cloacae* septic injury, 50 mL of an overnight
532 culture of bacteria was centrifuged 30 min at 3 000 x g. The supernatant was removed and
533 pellet used to infect the flies. For *E. faecalis* septic injury, overnight culture was diluted to
534 1/50 in fresh BHB and allowed to growth for 3 more hours at 37°C. The final culture was
535 centrifuged 10 min at 3000 x g and the pellet washed one time with sterile PBS. The bacteria
536 were resuspended to a final OD = 0.5 that was used to infect female flies with a septic injury.
537 3x 20 females were infected with each bacterium. The septic injury and the PBS clean injury
538 were performed as described (Haller et al., 2014): an electrolysis-sharpened tungsten wire
539 dipped or not in a microbial solution was used to prick flies in the thorax at a position
540 corresponding to alary muscles. 20 females were injured. For *B. bassiana* natural infection,
541 flies were anesthetized, deposited and shaken on a sporulating plate containing the fungus. 3
542 x 20 females were infected. Flies were kept at 29°C with 60% humidity and transferred,
543 without anesthesia, to fresh food every 2-3 days.

544

545 **Paraquat exposure**

546 Paraquat solution was prepared by dissolving Paraquat dichloride (Sigma-Aldrich # 50636) in
547 50 mM sucrose solution to obtain a final paraquat concentration at 1 mM. For survival test on
548 a paraquat supplemented sucrose only diet, 3x 20 female flies were fed on 2 mL on a 50 mM
549 sucrose plus 1 mM paraquat solution and kept at 25°C with 60% humidity.

550

551 **Dechorionation of *Drosophila* eggs**

552 Nora(+) flies were allowed to lay eggs overnight at 25°C in a cage on apple juice agar plate
553 with yeast paste in the center of the plate. Eggs were collected, washed with water, and
554 dechorionated with a 50% bleach solution for 3 min with constant up and down pipetting of
555 the solution. Eggs were abundantly rinsed with water, aligned under the microscope on a
556 piece of agar medium and transferred by capillarity on a coverslip. One drop of mineral oil
557 was applied to cover the eggs, and the coverslip was deposited on a petri dish with normal
558 *Drosophila* food. After 2 days, larvae were transferred to normal food vial (single bleaching)
559 or treated again with bleach solution as previously and then transferred to normal food vial
560 (double bleaching or even triple bleaching if needed). Once flies emerged, they were tested
561 for Nora virus infection. Usually, there was no difference in the results obtained with the
562 single or double bleaching procedures although this observation applies only to short term
563 observations.

564

565 **Pure Nora virus suspension preparation**

566 Nora(+) flies (around 5 000 flies) were crashed in ice cold PBS using a potter homogenizer.
567 The homogenate (around 35 mL) was transferred in a 50 mL Falcon tube and centrifuged at 1
568 500 rpm for 10 min, at 4°C in an Eppendorf 5810R centrifuge to remove wings, legs and
569 other fly debris. The resulting supernatant was sequentially filtrated through 0.8, 0.45 and

570 0.22 µm filter units and stored at -80°C. The homogenate (around 26 mL) was then layered in
571 two 15 ml Beckmann Ultra-Clear centrifuge tubes over 1.5 mL of a 30 % (wt/wt) sucrose
572 solution (50 mM Hepes pH 7.0, 0.1 % BSA) and centrifuged at 24,000 rpm for 6.5 hours at
573 11°C using a JS-24.15 rotor (Beckmann). The pellets were resuspended in a total volume of
574 500 µL Hepes solution (Hepes 50 mM, pH 7.0) and transferred into a 1.5 mL Eppendorf tube.
575 The solution was then centrifuged at 10,000 rpm for 10 min in a 5424 Eppendorf centrifuge
576 to discard insoluble material. The resulting supernatant containing virus particles was layered
577 over a 40-10 % (wt/wt) sucrose gradient (50 mM Hepes, pH 7.0) prepared in a 15 mL Ultra-
578 Clear centrifuge tube (Beckmann) and centrifuged at 11°C for 4h at 24,000 rpm in a JS-24.15
579 rotor (Beckmann). An opalescent band, that migrated near the middle of the tube, containing
580 virus particles was then collected by puncturing the tube with a 25-gauge needle mounted on
581 a 1 ml syringe. This solution was then layered onto a 30 % (wt/wt) sucrose solution contained
582 in a 15 mL Beckmann Ultra-Clear centrifuge tubes (50 mM Hepes pH 7.0, 0.1 % BSA) and
583 centrifuged at 24,000 rpm for 6.5 hours at 11°C using a JS-24.15 rotor (Beckmann). The
584 pellet was resuspended in 500 µl of Tris solution (Tris-HCl 10 mM, pH 7.5), aliquoted, and
585 stored at -80°C.
586
587 **Nora virus electronic microscopic picture**
588 The sample was prepared by plunge-freezing of 2.5 µL of the sample on a holey carbon
589 Quantifoil R 2/2 grid using FEI Vitrobot Mark IV machine. Images were gained on FEI
590 Polara F30 TEM microscope with acceleration voltage 100 KV and underfocus around 2.0
591 microns.
592
593 **Nora virus re-infection with the pure viral preparation**

594 Nora(-) flies were fed 24 hours with a 1/100 dilution of the viral preparation in sucrose
595 50mM. In practice, 200 µL of the 1/100 dilution (in sucrose 50mM) of the viral suspension
596 were deposited in an Eppendorf cup that was then placed in an empty fly tube. Flies (male
597 and females) were then added in the tube. The flies were allowed to feed on the viral
598 suspension for 24 hours and then transferred to a fly tube containing standard fly food.
599

600 **Nora virus re-infection with feces**

601 200 males of Nora(+) flies were allowed to deposit their feces in a food vial for 5 days at
602 25°C. Nora(+) flies were then replaced by 50 males and 50 females of cured Nora(+) flies.
603 After 5 days, the vial was emptied, and Nora virus infection status was monitored in those
604 flies (generation G0). Once the progeny emerged, 0 to 4 days old flies were transferred to a
605 fresh vial for 4 days and then monitored for Nora virus load or used for experiments (first
606 generation after re-infection G1). The same procedure was repeated with the second
607 generation after re-infection (G2).
608

609 **Generation of a polyclonal antibody that detects the Nora virus**

610 Pure virus preparation was mixed with complete (first inoculation) then incomplete Freund's
611 adjuvant and was injected intraperitoneally in BALB/c mice every week over a period of
612 three weeks prior to ultimately bleeding the mice. The specificity of the antibody was
613 assessed by immunohistochemistry on Nora-negative and Nora-positive flies as determined
614 using RTqPCR.
615

616 **Immunostainings**

617 Midguts were dissected in PBS and fixed for 30 minutes with 4% paraformaldehyde.
618 Samples were washed three times with PBS-Triton X-100 0.1% (PBT 0.1%) as described

619 (Socha et al., 2023). For actin staining midguts were incubated for 1h30 at room-temperature
620 or overnight at 4°C in 10 µM Fluorescein Isothiocyanate (FITC) (Sigma-Aldrich #P5282) or
621 Texas-Red labeled phalloidin (Invitrogen TM #T7471). Samples were then washed three
622 times with PBT 0.1%. All samples were mounted on diagnostic microscope slides (Thermo
623 Fisher Scientific) with Vectashield plus DAPI (Vector Laboratories). Samples were observed
624 using a LSM780 confocal microscope (Zeiss) or in Axioskop 2 microscope (Zeiss). All
625 images were analyzed with the ImageJ/Fiji software.
626
627 **Phospho-histone H3 immunostaining and microscopy**
628 Fly guts were dissected, fixed, stained by immunohistochemistry with an anti-pH3 antibody
629 (Millipore) and mounted following standard procedures (Lee et al., 2016). Midguts were
630 observed using a fluorescent microscope (Axioskop 2, ZEISS) and nuclei positive for pH3
631 staining were counted manually.
632
633 **Microbiota quantification**
634 Female flies were sterilized for 30 seconds in 70% ethanol and midguts were dissected in
635 sterile PBS (10 midguts per sample) and immediately transferred in sterile PBS. Midguts
636 were homogenized with a sterile pestle. Serial dilutions of the suspension were performed
637 prior to plating on specific solid media and incubated at 30°C. *Acetobacteriaceae* plates,
638 *Enterobacteriaceae* plates and MRS plates were performed as described (Guo et al., 2014).
639 For BHB agar plates: 37 g/L BHB (Sigma), 15 g/L agar (Sigma). Media were autoclaved 15
640 min, at 121°C (prior to use) and stored at 4°C.
641
642 **Bacterial titer in the hemolymph**

643 PA14 presence in the hemolymph was assessed as described previously (Haller et al., 2014);
644 briefly, hemolymph was collected by capillarity using a drawn-out pipette mounted on the
645 Nanoject II microinjector in the absence of oil. Hemolymph from 10 female flies per sample
646 was used.
647
648 **RT-qPCR analysis of gene expression in *Drosophila* midgut**
649 Fly midguts (without crop, hindgut and Malpighian tubules) were dissected (20 per sample)
650 and RNAs were extracted in TRI Reagent®-RT as described (Lee et al., 2016). Reverse
651 transcription was performed using iScriptTM (BIO-RAD). Quantitative PCR was performed
652 using iQTM SYBR® Green (BIO-RAD) and a C1000TM Thermal Cycler (BIO-RAD)
653 device. Expression values were calculated using a standard curve (with genomic DNA) and
654 normalized to *rp49* expression level. Results presented the average ± SD of 3 independent
655 experiments (with biological duplicates or triplicates). See primer sequences in Table 1.
656
657 **RT-qPCR analysis of Nora virus load**
658 Whole flies (6 per sample) were frozen at -80°C. RNA extraction with a Nucleospin® RNA
659 kit (Macherey-Nagel), reverse transcription and quantitative PCR were performed as
660 described (Haller et al., 2014). Quantification values were calculated using a standard curve
661 obtained from serial dilutions of a plasmid carrying the Nora virus DNA sequence amplified
662 by the couple of primers used for the PCR. See primer sequences in Table 1.
663 To check the absence of other potentially contaminating viruses in the purified Nora virus
664 preparations, we used the set of primers described by (Wu et al., 2010).
665
666 **Antibiotics treatment**

667 3x 20 female flies (3-8 days old) were kept on a sucrose (50mM) only diet with addition of a
668 5 antibiotics cocktail: 100 µg/mL ampicillin, 50 µg/mL vancomycin, 100 µg/mL neomycin,
669 100 µg/mL metronidazole and 50 µg/mL tetracyclin. Tubes were changed every 3 days and
670 flies transferred without anesthesia.
671
672 **SMURF**
673 The SMURF assay was developed to observe the integrity of the intestinal barrier (Rera et al.,
674 2011). Flies are kept on a sucrose solution colored with Blue food dye (Brilliant Blue FCF
675 E133). After ingestion, if there is an intestinal integrity loss, the dye will diffuse in the
676 hemolymph, coloring the fly in blue.
677
678 **ApopTAG**
679 Used as described by the manufacturer Sigma-Aldrich for the product ApopTag Fluorescein
680 In Situ Apoptosis Detection Kit.
681
682 **JAK-STAT gene expression**
683 Fly midguts (without crop, hindgut and Malpighian tubules) were dissected (20 per sample)
684 and RNAs were extracted in TRI Reagent®-RT as described (Lee et al., 2016). Reverse
685 transcription was performed using iScriptTM (BIO-RAD). Quantitative PCR was performed
686 using iQTM SYBR® Green (BIO-RAD) and a C1000TM Thermal Cycler (BIO-RAD)
687 device. Expression values were calculated using a standard curve (with genomic DNA) and
688 normalized to *rp49* expression level. Results presented the average ± SD of 3 independent
689 experiments (with biological duplicates or triplicates).
690
691 **Statistical analysis and reproducibility**

692 All statistical analyses were performed on Graphpad Prism version 10 (Graphpad software
693 Inc., San Diego, CA). The Mann–Whitney tests were used unless otherwise indicated. For
694 survival experiments, the time it takes for 50% of the flies to succumb (LT50) was
695 determined for each curve being compared. An unpaired *t*-test used on the LT50s from
696 biological triplicates was used to assess the significance between two survival curves. When
697 using parametric tests (analysis of variance (ANOVA) and *t*-test), a Gaussian distribution of
698 data was checked using either D'Agostino-Pearson omnibus, Anderson-Darling, or Shapiro-
699 Wilk normality tests. All experiments were performed at least three times. Significance
700 values: $*p < 0.05$, $**p < 0.01$, $***p < 0.001$, $****p < 0.0001$.
701

Acknowledgements

We thank Pr. JL. Imler for continuous support of this project, Dr. S. Limmer, Dr. A. Ayyaz, and J. Bourdeaux for early help with experiments, MC. Lacombe, and E. Santiago for expert technical assistance. We are also grateful to Dr. D. Rodrigues for checking the stability of ectopically expressed GFP in ISCs. SH has been funded by the University of Strasbourg (Présidence fellowship) and by a FRM 4th year Ph. D fellowship (FDT20130928220). VB was supported by a fellowship from MENRT. Dominique Ferrandon was leading a Équipe Fondation Recherche Médicale (FRM DEQ20090515394). This work has also been funded by Institutional funds from CNRS and by ANR (DROSOGUT), NIH (PO1 AI070167), the Investissement d'Avenir program Laboratoire d'Excellence (NetRNA ANR-10-LABX-36; I2MC ANR-11-EQPX-0022).

References

Ai, X., Deng, H., Li, X., Wei, Z., Chen, Y., Yin, T., Zhang, J., Huang, J., Li, H., Lin, X., *et al.* (2024). cGAS-like receptors drive a systemic STING-dependent host response in Drosophila. Cell reports *43*, 115081.

Apidianakis, Y., Pitsouli, C., Perrimon, N., and Rahme, L. (2009). Synergy between bacterial infection and genetic predisposition in intestinal dysplasia. Proc Natl Acad Sci U S A *106*, 20883-20888.

Arias-Rojas, A., and Iatsenko, I. (2022). The Role of Microbiota in Drosophila melanogaster Aging. Front Aging *3*, 909509.

Ayyaz, A., and Jasper, H. (2013). Intestinal inflammation and stem cell homeostasis in aging Drosophila melanogaster. Front Cell Infect Microbiol *3*, 98.

Biteau, B., Hochmuth, C.E., and Jasper, H. (2008). JNK activity in somatic stem cells causes loss of tissue homeostasis in the aging Drosophila gut. Cell Stem Cell *3*, 442-455.

Bonfini, A., Liu, X., and Buchon, N. (2016). From pathogens to microbiota: How Drosophila intestinal stem cells react to gut microbes. Dev Comp Immunol *64*, 22-38.

Borensztejn, A., Boissoneau, E., Fernandez, G., Agnes, F., and Pret, A.M. (2013). JAK/STAT autocontrol of ligand-producing cell number through apoptosis. Development *140*, 195-204.

Broderick, N.A., and Lemaitre, B. (2012). Gut-associated microbes of Drosophila melanogaster. Gut Microbes *3*, 307-321.

Buchon, N., Broderick, N.A., Chakrabarti, S., and Lemaitre, B. (2009a). Invasive and indigenous microbiota impact intestinal stem cell activity through multiple pathways in Drosophila. Genes Dev *23*, 2333-2344.

Buchon, N., Broderick, N.A., Poidevin, M., Pradervand, S., and Lemaitre, B. (2009b). Drosophila intestinal response to bacterial infection: activation of host defense and stem cell proliferation. Cell Host Microbe *5*, 200-211.

Buchon, N., Osman, D., David, F.P., Fang, H.Y., Boquete, J.P., Deplancke, B., and Lemaitre, B. (2013). Morphological and molecular characterization of adult midgut compartmentalization in Drosophila. Cell Rep *3*, 1725-1738.

Cai, H., Holleufer, A., Simonsen, B., Schneider, J., Lemoine, A., Gad, H.H., Huang, J., Huang, J., Chen, D., Peng, T., *et al.* (2020). 2'3'-cGAMP triggers a STING- and NF-kappaB-dependent broad antiviral response in Drosophila. Sci Signal *13*.

Chakrabarti, S., and Visweswariah, S.S. (2020). Intramacrophage ROS Primes the Innate Immune System via JAK/STAT and Toll Activation. Cell Rep *33*, 108368.

Chatterjee, M., and Ip, Y.T. (2009). Pathogenic stimulation of intestinal stem cell response in Drosophila. J Cell Physiol *220*, 664-671.

Chen, J., Lin, G., Ma, K., Guo, Y., Li, Z., Wang, X., and Ferrandon, D. (2025). N-acetyl-glucosamine primes Pseudomonas aeruginosa for virulence through a type IV pili/cAMP-mediated morphology transition. Nature communications *16*, 9405.

Chen, J., Lin, G., Ma, K., Li, Z., Liegeois, S., and Ferrandon, D. (2024). A specific innate immune response silences the virulence of Pseudomonas aeruginosa in a latent infection model in the Drosophila melanogaster host. PLoS Pathog *20*, e1012252.

Choi, N.H., Kim, J.G., Yang, D.J., Kim, Y.S., and Yoo, M.A. (2008). Age-related changes in Drosophila midgut are associated with PVF2, a PDGF/VEGF-like growth factor. Aging Cell *7*, 318-334.

Cronin, S.J., Nehme, N.T., Limmer, S., Liegeois, S., Pospisilik, J.A., Schramek, D., Leibbrandt, A., Simoes Rde, M., Gruber, S., Puc, U., *et al.* (2009). Genome-wide RNAi screen identifies genes involved in intestinal pathogenic bacterial infection. Science *325*, 340-343.

759 Donelick, H.M., Talide, L., Bellet, M., Aruscavage, P.J., Lauret, E., Aguiar, E., Marques, J.T., Meignin, C.,
760 and Bass, B.L. (2020). In vitro studies provide insight into effects of Dicer-2 helicase mutations in
761 Drosophila melanogaster. RNA *26*, 1847-1861.

762 Ekstrom, J.O., Habayeb, M.S., Srivastava, V., Kieselbach, T., Wingsle, G., and Hultmark, D. (2011).
763 Drosophila Nora virus capsid proteins differ from those of other picorna-like viruses. Virus Res *160*, 51-58.

764 Ekstrom, J.O., and Hultmark, D. (2016). A Novel Strategy for Live Detection of Viral Infection in
765 Drosophila melanogaster. Sci Rep *6*, 26250.

766 Ferrandon, D. (2013). The complementary facets of epithelial host defenses in the genetic model organism
767 Drosophila melanogaster: from resistance to resilience. Curr Opin Immunol *25*, 59-70.

768 Ferreira, A.G., Naylor, H., Esteves, S.S., Pais, I.S., Martins, N.E., and Teixeira, L. (2014). The Toll-dorsal
769 pathway is required for resistance to viral oral infection in Drosophila. PLoS Pathog *10*, e1004507.

770 Feuer, R., and Whitton, J.L. (2008). Preferential coxsackievirus replication in proliferating/activated cells:
771 implications for virus tropism, persistence, and pathogenesis. Curr Top Microbiol Immunol *323*, 149-173.

772 Galiana-Arnoux, D., Dostert, C., Schneemann, A., Hoffmann, J.A., and Imler, J.L. (2006). Essential
773 function in vivo for Dicer-2 in host defense against RNA viruses in drosophila. Nat Immunol *7*, 590-597.

774 Girardi, E., Lefevre, M., Chane-Woon-Ming, B., Paro, S., Claydon, B., Imler, J.L., Meignin, C., and
775 Pfeffer, S. (2015). Cross-species comparative analysis of Dicer proteins during Sindbis virus infection. Sci
776 Rep *5*, 10693.

777 Goto, A., Okado, K., Martins, N., Cai, H., Barbier, V., Lamiable, O., Troxler, L., Santiago, E., Kuhn, L.,
778 Paik, D*., et al.* (2020). The Kinase IKKbeta Regulates a STING-and NF-kappaB-Dependent Antiviral
779 Response Pathway in Drosophila. Immunity *52*, 200.

780 Guo, L., Karpac, J., Tran, S.L., and Jasper, H. (2014). PGRP-SC2 promotes gut immune homeostasis to
781 limit commensal dysbiosis and extend lifespan. Cell *156*, 109-122.

782 Habayeb, M.S., Cantera, R., Casanova, G., Ekstrom, J.O., Albright, S., and Hultmark, D. (2009a). The
783 Drosophila Nora virus is an enteric virus, transmitted via feces. J Invertebr Pathol *101*, 29-33.

784 Habayeb, M.S., Ekengren, S.K., and Hultmark, D. (2006). Nora virus, a persistent virus in Drosophila,
785 defines a new picorna-like virus family. J Gen Virol *87*, 3045-3051.

786 Habayeb, M.S., Ekstrom, J.O., and Hultmark, D. (2009b). Nora virus persistent infections are not affected
787 by the RNAi machinery. PLoS One *4*, e5731.

788 Haller, S., Franchet, A., Hakkim, A., Chen, J., Drenkard, E., Yu, S., Schirmeier, S., Li, Z., Martins, N.,
789 Ausubel, F.M*., et al.* (2018). Quorum-sensing regulator RhlR but not its autoinducer RhlI enables
790 Pseudomonas to evade opsonization. EMBO Rep *19*, e44880.

791 Haller, S., Limmer, S., and Ferrandon, D. (2014). Assessing Pseudomonas virulence with a nonmammalian
792 host: Drosophila melanogaster. Methods Mol Biol *1149*, 723-740.

793 Hanson, M.A., and Lemaitre, B. (2023). Antimicrobial peptides do not directly contribute to aging in
794 Drosophila, but improve lifespan by preventing dysbiosis. Dis Model Mech *16*, dmm049965.

795 Hay, B.A., Wolff, T., and Rubin, G.M. (1994). Expression of baculovirus P35 prevents cell death in
796 Drosophila. Development *120*, 2121-2129.

797 Herrera, S.C., and Bach, E.A. (2019). JAK/STAT signaling in stem cells and regeneration: from
798 Drosophila to vertebrates. Development *146*, 167643.

799 Hodgson, J.J., Chen, R.Y., Blissard, G.W., and Buchon, N. (2024). Viral and cellular determinants of
800 polarized trafficking of viral envelope proteins from insect-specific and insect-vectored viruses in insect
801 midgut and salivary gland cells. J Virol *98*, e0054024.

802 Iatsenko, I., Boquete, J.P., and Lemaitre, B. (2018). Microbiota-Derived Lactate Activates Production of
803 Reactive Oxygen Species by the Intestinal NADPH Oxidase Nox and Shortens Drosophila Lifespan.
804 Immunity *49*, 929-942 e925.

805 Jiang, H., and Edgar, B.A. (2011). Intestinal stem cells in the adult Drosophila midgut. Exp Cell Res *317*,
806 2780-2788.

807 Jiang, H., Patel, P.H., Kohlmaier, A., Grenley, M.O., McEwen, D.G., and Edgar, B.A. (2009).
808 Cytokine/Jak/Stat signaling mediates regeneration and homeostasis in the Drosophila midgut. Cell *137*,
809 1343-1355.

810 Jones, R.M., Luo, L., Ardita, C.S., Richardson, A.N., Kwon, Y.M., Mercante, J.W., Alam, A., Gates, C.L.,
811 Wu, H., Swanson, P.A., *et al.* (2013). Symbiotic lactobacilli stimulate gut epithelial proliferation via Nox-
812 mediated generation of reactive oxygen species. EMBO J *32*, 3017-3028.

813 Jung, A., Criqui, M.-C., Rutschmann, S., Hoffmann, J.-A., and Ferrandon, D. (2001). A microfluorometer
814 assay to measure the expression of ß-galactosidase and GFP reporter genes in single *Drosophila* flies.
815 Biotechniques *30*, 594-601.

816 Kim, S.H., and Lee, W.J. (2014). Role of DUOX in gut inflammation: lessons from Drosophila model of
817 gut-microbiota interactions. Front Cell Infect Microbiol *3*, 116.

818 Lee, K.Z., Lestradet, M., Socha, C., Schirmeier, S., Schmitz, A., Spenle, C., Lefebvre, O., Keime, C.,
819 Yamba, W.M., Bou Aoun, R., *et al.* (2016). Enterocyte Purge and Rapid Recovery Is a Resilience Reaction
820 of the Gut Epithelium to Pore-Forming Toxin Attack. Cell Host Microbe *20*, 716-730.

821 Lemaitre, B., and Miguel-Aliaga, I. (2013). The digestive tract of Drosophila melanogaster. Annu Rev
822 Genet *47*, 377-404.

823 Lemaitre, B., Reichhart, J.M., and Hoffmann, J.A. (1997). Drosophila host defense: differential induction
824 of antimicrobial peptide genes after infection by various classes of microorganisms. Proc Natl Acad Sci U
825 S A *94*, 14614-14619.

826 Lestradet, M., Lee, K.Z., and Ferrandon, D. (2014). Drosophila as a model for intestinal infections.
827 Methods Mol Biol *1197*, 11-40.

828 Lian, S., Liu, J., Wu, Y., Xia, P., and Zhu, G. (2022). Bacterial and Viral Co-Infection in the Intestine:
829 Competition Scenario and Their Effect on Host Immunity. International journal of molecular sciences *23*,
830 2311.

831 Limmer, S., Haller, S., Drenkard, E., Lee, J., Yu, S., Kocks, C., Ausubel, F.M., and Ferrandon, D. (2011).
832 Pseudomonas aeruginosa RhlR is required to neutralize the cellular immune response in a Drosophila
833 melanogaster oral infection model. Proc Natl Acad Sci U S A *108*, 17378-17383.

834 Liu, Z., Zhang, H., Lemaitre, B., and Li, X. (2024). Duox activation in Drosophila Malpighian tubules
835 stimulates intestinal epithelial renewal through a countercurrent flow. Cell Rep *43*, 114109.

836 Magwire, M.M., Fabian, D.K., Schweyen, H., Cao, C., Longdon, B., Bayer, F., and Jiggins, F.M. (2012).
837 Genome-wide association studies reveal a simple genetic basis of resistance to naturally coevolving
838 viruses in Drosophila melanogaster. PLoS Genet *8*, e1003057.

839 Maillard, P.V., Ciaudo, C., Marchais, A., Li, Y., Jay, F., Ding, S.W., and Voinnet, O. (2013). Antiviral
840 RNA interference in mammalian cells. Science *342*, 235-238.

841 Maillard, P.V., Van der Veen, A.G., Deddouche-Grass, S., Rogers, N.C., Merits, A., and Reis e Sousa, C.
842 (2016). Inactivation of the type I interferon pathway reveals long double-stranded RNA-mediated RNA
843 interference in mammalian cells. EMBO J *35*, 2505-2518.

844 Medzhitov, R., Schneider, D.S., and Soares, M.P. (2012). Disease tolerance as a defense strategy. Science
845 *335*, 936-941.

846 Micchelli, C.A., and Perrimon, N. (2006). Evidence that stem cells reside in the adult Drosophila midgut
847 epithelium. Nature *439*, 475-479.

848 Mondotte, J.A., Gausson, V., Frangeul, L., Blanc, H., Lambrechts, L., and Saleh, M.C. (2018). Immune
849 priming and clearance of orally acquired RNA viruses in Drosophila. Nat Microbiol *3*, 1394-1403.

850 Nagai, H., Nagai, L.A.E., Tasaki, S., Nakato, R., Umetsu, D., Kuranaga, E., Miura, M., and Nakajima, Y.
851 (2023). Nutrient-driven dedifferentiation of enteroendocrine cells promotes adaptive intestinal growth in
852 Drosophila. Dev Cell *58*, 1764-1781 e1710.

853 Nehme, N.T., Liegeois, S., Kele, B., Giammarinaro, P., Pradel, E., Hoffmann, J.A., Ewbank, J.J., and
854 Ferrandon, D. (2007). A model of bacterial intestinal infections in Drosophila melanogaster. PLoS Pathog
855 *3*, e173.

856 Niehus, S., Giammarinaro, P., Liegeois, S., Quintin, J., and Ferrandon, D. (2012). Fly culture collapse
857 disorder: detection, prophylaxis and eradication of the microsporidian parasite Tubulinosema ratisbonensis
858 infecting Drosophila melanogaster. Fly (Austin) *6*, 193-204.

859 Nigg, J.C., Castello-Sanjuan, M., Blanc, H., Frangeul, L., Mongelli, V., Godron, X., Bardin, A.J., and
860 Saleh, M.C. (2024). Viral infection disrupts intestinal homeostasis via Sting-dependent NF-kappaB
861 signaling in Drosophila. Curr Biol *34*, 2785-2800 e2787.

862 Nigg, J.C., Mongelli, V., Blanc, H., and Saleh, M.C. (2022). Innovative Toolbox for the Quantification of
863 Drosophila C Virus, Drosophila A Virus, and Nora Virus. J Mol Biol *434*, 167308.

864 Ohlstein, B., and Spradling, A. (2006). The adult Drosophila posterior midgut is maintained by pluripotent
865 stem cells. Nature *439*, 470-474.

866 Patel, P.H., Penalva, C., Kardorff, M., Roca, M., Pavlovic, B., Thiel, A., Teleman, A.A., and Edgar, B.A.
867 (2019). Damage sensing by a Nox-Ask1-MKK3-p38 signaling pathway mediates regeneration in the adult
868 Drosophila midgut. Nature communications *10*, 4365.

869 Poirier, E.Z., Buck, M.D., Chakravarty, P., Carvalho, J., Frederico, B., Cardoso, A., Healy, L., Ulferts, R.,
870 Beale, R., and Reis e Sousa, C. (2021). An isoform of Dicer protects mammalian stem cells against
871 multiple RNA viruses. Science *373*, 231-236.

872 Rahmatika, D., Kuroda, N., Min, Z., Nainu, F., Nagaosa, K., and Nakanishi, Y. (2019). Inhibitory effects
873 of viral infection on cancer development. Virology *528*, 48-53.

874 Rahme, L.G., Stevens, E.J., Wolfort, S.F., Shao, J., Tompkins, R.G., and Ausubel, F.M. (1995). Common
875 virulence factors for bacterial pathogenicity in plants and animals. Science *268*, 1899-1902.

876 Rera, M., Bahadorani, S., Cho, J., Koehler, C.L., Ulgherait, M., Hur, J.H., Ansari, W.S., Lo, T., Jr., Jones,
877 D.L., and Walker, D.W. (2011). Modulation of longevity and tissue homeostasis by the Drosophila PGC-1
878 homolog. Cell Metab *14*, 623-634.

879 Rogers, A., Towery, L., McCown, A., and Carlson, K.A. (2020). Impaired Geotaxis as a Novel Phenotype
880 of Nora Virus Infection of Drosophila melanogaster. Scientifica (Cairo) *2020*, 1804510.

881 Rutschmann, S., Jung, A.C., Hetru, C., Reichhart, J.M., Hoffmann, J.A., and Ferrandon, D. (2000). The
882 Rel protein DIF mediates the antifungal but not the antibacterial host defense in Drosophila. Immunity *12*,
883 569-580.

884 Sansone, C.L., Cohen, J., Yasunaga, A., Xu, J., Osborn, G., Subramanian, H., Gold, B., Buchon, N., and
885 Cherry, S. (2015). Microbiota-Dependent Priming of Antiviral Intestinal Immunity in Drosophila. Cell
886 Host Microbe *18*, 571-581.

887 Schissel, M., Best, R., Liesemeyer, S., Tan, Y.D., Carlson, D.J., Shaffer, J.J., Avuthu, N., Guda, C., and
888 Carlson, K.A. (2021). Effect of Nora virus infection on native gut bacterial communities of Drosophila
889 melanogaster. AIMS Microbiol *7*, 216-237.

890 Schneider, J., and Imler, J.L. (2021). Sensing and signalling viral infection in drosophila. Dev Comp
891 Immunol *117*, 103985.

892 Segrist, E., Dittmar, M., Gold, B., and Cherry, S. (2021). Orally acquired cyclic dinucleotides drive
893 dSTING-dependent antiviral immunity in enterocytes. Cell reports *37*, 110150.

894 Segrist, E., Miller, S., Gold, B., Li, Y., and Cherry, S. (2024). Tissue specific innate immune responses
895 impact viral infection in Drosophila. PLoS Pathog *20*, e1012672.

896 Sina Rahme, B., Lestradet, M., Di Venanzio, G., Ayyaz, A., Yamba, M.W., Lazzaro, M., Liegeois, S.,
897 Garcia Vescovi, E., and Ferrandon, D. (2022). The fliR gene contributes to the virulence of S. marcescens
898 in a Drosophila intestinal infection model. Scientific reports *12*, 3068.

899 Socha, C., Pais, I.S., Lee, K.Z., Liu, J., Liegeois, S., Lestradet, M., and Ferrandon, D. (2023). Fast
900 drosophila enterocyte regrowth after infection involves a reverse metabolic flux driven by an amino acid
901 transporter. iScience *26*, 107490.

902 Takeishi, A., Kuranaga, E., Tonoki, A., Misaki, K., Yonemura, S., Kanuka, H., and Miura, M. (2013).
903 Homeostatic epithelial renewal in the gut is required for dampening a fatal systemic wound response in
904 Drosophila. Cell Rep *3*, 919-930.

905 Tauszig-Delamasure, S., Bilak, H., Capovilla, M., Hoffmann, J.A., and Imler, J.L. (2002). Drosophila
906 MyD88 is required for the response to fungal and Gram-positive bacterial infections. Nat Immunol *3*, 91-
907 97.

908 Thibault, S.T., Singer, M.A., Miyazaki, W.Y., Milash, B., Dompe, N.A., Singh, C.M., Buchholz, R.,
909 Demsky, M., Fawcett, R., Francis-Lang, H.L.*, et al.* (2004). A complementary transposon tool kit for
910 Drosophila melanogaster using P and piggyBac. Nat Genet *36*, 283-287.

911 van Mierlo, J.T., Bronkhorst, A.W., Overheul, G.J., Sadanandan, S.A., Ekstrom, J.O., Heestermans, M.,
912 Hultmark, D., Antoniewski, C., and van Rij, R.P. (2012). Convergent evolution of argonaute-2 slicer
913 antagonism in two distinct insect RNA viruses. PLoS Pathog *8*, e1002872.

914 van Rij, R.P., Saleh, M.C., Berry, B., Foo, C., Houk, A., Antoniewski, C., and Andino, R. (2006). The
915 RNA silencing endonuclease Argonaute 2 mediates specific antiviral immunity in Drosophila
916 melanogaster. Genes Dev *20*, 2985-2995.

917 Webster, C.L., Waldron, F.M., Robertson, S., Crowson, D., Ferrari, G., Quintana, J.F., Brouqui, J.M.,
918 Bayne, E.H., Longdon, B., Buck, A.H.*, et al.* (2015). The Discovery, Distribution, and Evolution of
919 Viruses Associated with Drosophila melanogaster. PLoS Biol *13*, e1002210.

920 Wu, Q., Luo, Y., Lu, R., Lau, N., Lai, E.C., Li, W.X., and Ding, S.W. (2010). Virus discovery by deep
921 sequencing and assembly of virus-derived small silencing RNAs. Proc Natl Acad Sci U S A *107*, 1606-
922 1611.

923 Wu, X., Dao Thi, V.L., Huang, Y., Billerbeck, E., Saha, D., Hoffmann, H.H., Wang, Y., Silva, L.A.V.,
924 Sarbanes, S., Sun, T.*, et al.* (2018). Intrinsic Immunity Shapes Viral Resistance of Stem Cells. Cell *172*,
925 423-438 e425.

926 Wu, X., Kwong, A.C., and Rice, C.M. (2019). Antiviral resistance of stem cells. Curr Opin Immunol *56*,
927 50-59.

928 Xu, R., Lou, Y., Tidu, A., Bulet, P., Heinekamp, T., Martin, F., Brakhage, A., Li, Z., Liegeois, S., and
929 Ferrandon, D. (2023). The Toll pathway mediates Drosophila resilience to Aspergillus mycotoxins through
930 specific Bomanins. EMBO Rep *24*, e56036.

931 Zeng, X., Chauhan, C., and Hou, S.X. (2010). Characterization of midgut stem cell- and enteroblast-
932 specific Gal4 lines in drosophila. Genesis *48*, 607-611.

933 Zhou, F., Rasmussen, A., Lee, S., and Agaisse, H. (2013). The UPD3 cytokine couples environmental
934 challenge and intestinal stem cell division through modulation of JAK/STAT signaling in the stem cell
935 microenvironment. Dev Biol *373*, 383-393.

936

937 **Figures Legends**

938 **Figure 1. Correlation between Nora virus infection and impaired defense against *P.***
939 ***aeruginosa* intestinal infection as well as lowered fitness**

940 The Oregon-R sub-strain infected with Nora virus is referred to as Ore-R(SM), while the non-
941 infected sub-strain is referred to as Ore-R(SC). (**A**) Survival of Ore-R(SM) (Nora(+)) and
942 Ore-R(SC) (Nora(-)) flies following oral exposure to *P. aeruginosa* PA14 (OD 0.25) at 25 °C.
943 NI: not infected. (**B**) Lifespan analysis of Nora-infected and non-infected flies maintained
944 under standard laboratory conditions at 25 °C. (**C**) Nora virus RNA levels in Ore-R(SM) and
945 Ore-R(SC) stocks quantified by RT-qPCR. (**D**) Quantification of phospho-histone H3
946 (PHH3)-positive nuclei in the midgut of Ore-R(SM) (Nora(+)) and Ore-R(SC) (Nora(-)) flies
947 at 2 days following oral PA14 infection or in non-infected (NI) controls. PHH3-positive
948 nuclei counts were assessed as a measure of epithelial cell proliferation. (**E**) Nora virus RNA
949 levels measured by RT-qPCR in the original Ore-R(SM) stock and in stocks cured of Nora
950 virus by embryo bleaching. (**F**) Survival of uncured and cured Ore-R(SM) stocks to the
951 ingestion of PA14. Each graphic is representative of three independent experiments. Survival
952 panels are presented as mean ± SEM with each curve representing a triplicate of 20 flies.
953 Other panels are presented as box and whiskers where the middle bar of the box plots
954 represents the median, and the upper and lower limits of boxes indicate the first and third
955 quartiles, respectively; the whiskers define the minima and maxima. Each dot in Nora virus
956 load panels (C, E) represent a sample of 5 flies. Each dot in the PHH3 quantification panel (D)
957 represents one single posterior midgut. Survival data were analyzed using a log-rank (Mantel-
958 Cox) test. Nora virus load in (C) was analyzed using a Mann-Whitney nonparametric test.
959 PHH3 quantification (D) and Nora load (E) were analyzed using one-way ANOVA with
960 Tukey's post-hoc tests. Statistical significance is indicated as **$p < 0.01$, ***$p < 0.001$,
961 ****$p < 0.0001$.

962

963 **Figure 2. Infection of Nora(-) flies with the purified Nora virus recapitulates the fitness**
964 **properties of Nora naturally infected flies**

965 Flies used in these experiments were derived from Ore-R(SM) stocks cured of Nora virus by
966 egg bleaching. A subset of cured flies was experimentally re-infected with a purified Nora
967 virus preparation (Nora(+) re-inf virus), while control flies remained uninfected (Nora(-)).
968 PA14: infection with *P. aeruginosa* PA14; NI: noninfected. (**A**) Transmission electron
969 microscopy image of the purified Nora virus preparation used for re-infection. (**B**) Nora virus
970 RNA levels measured by RT-qPCR in Nora(+) and Nora(-) flies across successive
971 generations following experimental re-infection: G0 to G2. (**C**) Survival of re-infected
972 Nora(+) and Nora(-) flies following oral exposure to PA14 at 25 °C. (**D**) Quantification of
973 phospho-histone H3 (PHH3)-positive nuclei in the midgut of re-infected Nora(+) and Nora(-)
974 flies following two days of PA14 ingestion or in non-infected (NI) controls. (**E**) Lifespan
975 analysis of Nora(+) and Nora(-) flies maintained under standard laboratory conditions at
976 29 °C. (**F**) Lifespan analysis of re-infected Nora(+) and Nora(-) flies maintained on a
977 sucrose-only diet at 25 °C. Each graphic is representative of three independent experiments.
978 Survival panels are presented as mean ± SEM with each curve representing a triplicate of 20
979 flies. Other panels are presented as box and whiskers where the middle bar of the box plots
980 represents the median, and the upper and lower limits of boxes indicate the first and third
981 quartiles, respectively; the whiskers define the minima and maxima. Each dot in the Nora
982 virus load panel (B) represents a sample of 5 flies. Each dot in the PHH3 quantification panel
983 (D) represents one single posterior midgut. Survival data were analyzed using a log-rank
984 (Mantel-Cox) test. Nora virus load was analyzed using a Mann-Whitney nonparametric test
985 (B). PHH3 quantification (D) was analyzed using one-way ANOVA with Tukey's post-hoc
986 test. Statistical significance is indicated as ***$p < 0.001$, ****$p < 0.0001$.

987

988 **Figure 3. Influence of age, diet, and microbiota on Nora virus load and fly fitness**

989 (**A**) Nora virus RNA levels measured by RT-qPCR at 3 days following oral exposure to *P.*
990 *aeruginosa* PA14 in Nora-infected and non-infected flies maintained on either standard diet
991 or rich diet (standard medium supplemented with 5x yeast). (**B**) Nora virus RNA levels
992 measured by RT-qPCR in young (3-day-old) and aged (30-day-old) Nora-infected flies. (**C**)
993 Quantification of total culturable bacterial microbiota by colony-forming unit (CFU) counts
994 in young Nora(+) and Nora(-) flies maintained for 8 days on a sucrose-only diet, and in aged
995 flies maintained on standard fly food. CFU values are presented on a logarithmic scale. (**D**)
996 Lifespan analysis of Nora-infected (Nora(+) and non-infected (Nora(-) flies maintained on
997 standard diet in the presence or absence of antibiotics (ABX). (**E**) Lifespan analysis of Nora-
998 infected (+) and non-infected (-) flies maintained on rich diet in the presence or absence of
999 antibiotics (ABX). Each graphic is representative of three independent experiments. Survival
1000 panels are presented as mean ± SEM with each curve representing a triplicate of 20 flies.
1001 Other panels are presented as box and whiskers where the middle bar of the box plots
1002 represents the median, and the upper and lower limits of boxes indicate the first and third
1003 quartiles, respectively; the whiskers define the minima and maxima. Relative unit was used
1004 for Nora virus load panels. Each dot in Nora virus load panels (A, B) represent a sample of 5
1005 flies. Each dot in the CFU quantification panel (C) represents one single posterior midgut
1006 microbiota. Survival data were analyzed using a log-rank (Mantel-Cox) test. Nora virus load
1007 was analyzed using a Mann-Whitney nonparametric test (A, B). CFU quantification was
1008 analyzed using one-way ANOVA with Tukey's post-hoc test (C). Statistical significance is
1009 indicated as *$p < 0.05$, **$p < 0.01$, ****$p < 0.0001$.

1010

1011 **Figure 4. Alterations in intestinal barrier integrity and systemic bacterial dissemination**
1012 **in Nora virus-infected flies**

1013 (**A**) Representative images from the SMURF assay in 30-day-old non-infected fly (top) and
1014 Nora-infected fly (bottom) fed on a sucrose solution containing a blue dye. (**B**) Quantification
1015 of SMURF-positive Nora(-) or Nora (+) flies at 30 days of age maintained on rich diet
1016 (standard medium supplemented with 5x yeast) (**C**) Representative LB agar plate showing
1017 bacterial growth from serial dilutions of hemolymph collected from non-infected flies and
1018 from Nora-infected flies exhibiting either SMURF-negative or SMURF-positive phenotypes.
1019 Age of flies corresponding to the LT50 observed in the survival assay shown in Fig. 3E
1020 (Nora(-): 65 days; Nora(+): 30 days). (**D**) Quantification of bacterial titers in the hemolymph
1021 at 3 days following oral exposure to *P. aeruginosa* PA14 in Nora-infected and non-infected
1022 flies. (**E**) Relative expression of the antimicrobial peptide gene *Diptericin* in dissected
1023 midguts of Nora(+) flies measured by RT-qPCR following 2 days of PA14 intestinal
1024 infection or after feeding with 1% SDS for 4-6 hours. Each graphic is representative of three
1025 independent experiments. All panels are presented as box and whiskers where the middle bar
1026 of the box plots represents the median, and the upper and lower limits of boxes indicate the
1027 first and third quartiles, respectively; the whiskers define the minima and maxima. Each dot
1028 in the SMURF quantification panel (A) represents a single SMURF-positive fly. Each dot in
1029 the CFU quantification panel (C) represents one single fly hemolymph bacterial titer. Each
1030 dot in the *Diptericin* gene expression panel represents a sample of 5 midguts. The percentage
1031 of SMURF-positive flies was analyzed using a Mann-Whitney nonparametric test (B). CFU
1032 counts (D) and *Diptericin* gene expression levels (E) were analyzed using one-way ANOVA
1033 with Tukey's post-hoc test. Statistical significance is indicated as *$p < 0.05$, ****$p < 0.0001$.
1034

1035 **Figure 5. Nora virus is initially found in intestinal progenitor cells and is also located in**
1036 **enterocytes upon infectious or chemical stresses**
1037 (**A**) Nora virus RNA levels measured by RT-qPCR in whole flies or in dissected intestines.
1038 (**B**) Representative confocal images of intestines from 5-day-old non-infected flies. Tissues
1039 were fixed and stained for DNA (DAPI, blue), actin (FITC, green), and Nora virus (Cy3, red).
1040 The Cy3 secondary antibody (goat anti-mouse) shows background signal in intestinal
1041 muscles. Scale bar, 5 µm. (**C**) Representative confocal images of intestines from 5-day-old
1042 Nora-infected flies stained for DNA (DAPI, blue), actin (FITC, green), and Nora virus (Cy3,
1043 red). Scale bars, 3 µm (left) and 5 µm (right). (**D**) Colocalization analysis of Nora virus signal
1044 with progenitor cells marked using the *esg-Gal4, Gal80^{ts}* driver crossed to *UAS-GFP*.
1045 Intestines were fixed and stained for DNA (DAPI, blue) and Nora virus (Cy3, red) Scale bars,
1046 2 µm (left) and 5 µm (right). (**E**) Representative confocal images of intestines from Nora-
1047 infected *GFP::Dicer-2* flies stained for DNA (DAPI, blue), actin (RFP, red), Dicer-2 (GFP,
1048 green), and Nora virus (Cy5, purple). Scale bars, 10 µm (left) and 5 µm (right). (**F**) Survival
1049 analysis of Nora-infected (+) and non-infected flies (-) following intestinal infection with *P.*
1050 *aeruginosa* PA14 (OD 0.25) or *S. marcescens* Db11 (OD 0.25), or exposure to 1 mM
1051 paraquat. (**G**) Nora virus RNA levels measured by RT-qPCR in flies from the experimental
1052 conditions shown in (F). (**H**) Representative confocal images of intestines from Nora-infected
1053 flies following PA14 infection, Db11 infection, or paraquat exposure. Tissues were fixed and
1054 stained for DNA (DAPI, blue), actin (FITC, green), and Nora virus (Cy3, red). Scale bar, 3
1055 µm. (**I**) Quantification of (H). EC: enterocyte; ISC: progenitor cells. Each graphic is
1056 representative of three independent experiments. Survival panels are presented as mean ±
1057 SEM with each curve representing a triplicate of 20 flies. Other panels are presented as box
1058 and whiskers where the middle bar of the box plots represents the median, and the upper and
1059 lower limits of boxes indicate the first and third quartiles, respectively; the whiskers define

1060 the minima and maxima. Relative unit was used for Nora virus load panels. Each dot in Nora
1061 virus load panels (A, G) represent a sample of 5 flies. Survival data were analyzed using a
1062 log-rank (Mantel-Cox) test. Nora virus load was analyzed using a Mann-Whitney
1063 nonparametric test (A). Comparisons of Nora virus load under pathogen infection or paraquat
1064 exposure (G) and of quantification of Nora (+) ECs (I) were analyzed using one-way
1065 ANOVA with Tukey's post-hoc test. Statistical significance is indicated as *$p < 0.05$, **$p <$
1066 0.01, ***$p < 0.001$, ****$p < 0.0001$.
1067
1068 **Figure 6. Inhibition of apoptosis prevents epithelial turnover and the proliferation of**
1069 **Nora virus**
1070 (**A**) Quantification of apoptotic nuclei in the posterior midgut (region R4 & R5 [see Fig. S5J])
1071 using ApopTag staining following *P. aeruginosa* PA14 infection or 1 mM paraquat exposure
1072 and controls. (**B**) Quantification of phospho-histone H3 (PHH3)-positive nuclei in the
1073 posterior midgut of Nora-infected flies 24h after PA14 infection or paraquat exposure. (**C**)
1074 Survival analysis of non-infected flies (Nora(-)) following PA14 intestinal infection (+ PA14)
1075 in control genotypes (NPG4G80 driver: [*NP1-Gal4, Gal80*^{ts}] and *UAS-p35* alone) and in flies
1076 with enterocyte expression of the apoptosis inhibitor gene *p35* (*NP>p35*). (**D**) Survival
1077 analysis of Nora-infected flies (Nora(+)) following PA14 intestinal infection in control
1078 genotypes and in flies expressing the *p35* gene in the intestine. (**E**) Quantification of PHH3-
1079 positive nuclei in the posterior midgut at 5 days following PA14 infection in flies from panels
1080 (C) and (D). PHH3-positive nuclei were quantified in control and apoptosis-inhibited
1081 intestines. (**F**) Nora virus RNA levels measured by RT-qPCR at 3 days following PA14
1082 infection in intestines from flies shown in (D). (**G**) Representative confocal images of old
1083 intestines (30-day-old) from Nora-infected flies in control genotypes (*NP* driver (NPG4G80)
1084 and *UAS-p35* alone) and in flies expressing p35 in the intestine (*NP>p35*). Tissues were fixed

1085 and stained for DNA (DAPI, blue), actin (FITC, green), and Nora virus (Cy3, red). Scale bar,
1086 5 µm. (**H**) Quantification of Nora virus-positive cells in the intestine from the experimental
1087 conditions shown in (G). Each graphic is representative of three independent experiments.
1088 Survival panel is presented as mean ± SEM with each curve representing a triplicate of 20
1089 flies. Other panels are presented as box and whiskers where the middle bar of the box plots
1090 represents the median, and the upper and lower limits of boxes indicate the first and third
1091 quartiles, respectively; the whiskers define the minima and maxima. Relative unit was used
1092 for Nora virus load panels. Each dot in Nora virus load panel (F) represents a sample of 5
1093 flies. Each dot in the PHH3 quantification panels (B, E) represent one single posterior midgut.
1094 Each dot in the ApopTag quantification panel (A) represents one single posterior midgut.
1095 Each dot in the Nora virus quantification panel (H) represents a region of one single posterior
1096 midgut. Survival data were analyzed using a log-rank (Mantel-Cox) test. ApopTag, PHH3,
1097 and Nora virus quantifications were analyzed using one-way ANOVA with Tukey's post-hoc
1098 test (A, B, E, F, H). Statistical significance is indicated as *$p < 0.05$, **$p < 0.01$, ***$p <$
1099 0.001, ****$p < 0.0001$.
1100
1101 **Figure 7. Inhibition of the JAK-STAT pathway prevents epithelial turnover and the**
1102 **proliferation of Nora virus**
1103 (**A-B**) Survival analysis of non-infected flies (A) and infected flies (B) following *P.*
1104 *aeruginosa* PA14 intestinal infection of flies in which RNAi-mediated silencing of JAK-
1105 STAT pathway component genes (*domeless* and *Stat92E*) in intestinal stem cells was
1106 achieved using the *Delta* driver. Control genotypes and non-infected (NI) survival assays are
1107 shown in the lower right insets. (**C**) Relative expression of JAK-STAT pathway-related genes
1108 (*upd3*, *dome*, *STAT92E*, *SOCS36E*, and *PIAS*) measured by RT-qPCR at 3 days following
1109 PA14 infection in Nora-infected (+) and non-infected (-) flies' midguts. (**D**) Quantification of

1110 *upd3-GFP* reporter signal in the posterior midgut at 2 days following PA14 infection in
1111 Nora-infected (+) and non-infected (-) flies. (**E**) Quantification of phospho-histone H3
1112 (PHH3)-positive nuclei in the posterior midgut at 3 days following PA14 infection in flies
1113 with RNAi-mediated silencing of *domeless* or *Stat92E* in intestinal stem cells using the
1114 *Delta-Gal4* driver. PHH3-positive nuclei were used as a measure of epithelial proliferation.
1115 (**F**) Nora virus RNA levels measured by RT-qPCR in intestines from flies shown in (E). (**G**)
1116 Representative confocal images of intestines from Nora-infected flies in control genotypes
1117 (*Delta>control RNAi*) and *UAS-p35* alone) and in flies expressing p35 in the intestine
1118 (*NP>p35*). Tissues were fixed and stained for DNA (DAPI, blue), actin (FITC, green), and
1119 Nora virus (Cy3, red). Scale bar, 5 µm. (**H**) Quantification of Nora-positive cells of the
1120 intestinal epithelium displayed in (G). EC: enterocyte; ISC: progenitor cells. Each graphic is
1121 representative of three independent experiments. Survival panels are presented as mean ±
1122 SEM with each curve representing a triplicate of 20 flies. Other panels are presented as box
1123 and whiskers where the middle bar of the box plots represents the median, and the upper and
1124 lower limits of boxes indicate the first and third quartiles, respectively; the whiskers define
1125 the minima and maxima. Relative unit was used for Nora virus load panels. Each dot in Nora
1126 virus load panel (F) represents a sample of 5 flies. Each dot in the PHH3 quantification
1127 panels (E) represent one single posterior midgut. Each dot in the gene expression panel (C)
1128 represents 5 posterior midguts. Each dot in the upd3-GFP quantification panel (D) represents
1129 one single posterior midgut. Survival data (A-B) were analyzed using a log-rank (Mantel-Cox)
1130 test. PHH3 quantification (E), gene expression analysis (C), upd3-GFP quantification (D),
1131 Nora virus load (F), and the number of Nora (+) enterocytes (H) were analyzed using one-
1132 way ANOVA with Tukey's post-hoc test. Statistical significance is indicated as *$p < 0.05$,
1133 **$p < 0.01$, ***$p < 0.001$, ****$p < 0.0001$.
1134

1135 **Figure 8: Model of Nora virus propagation in *Drosophila* intestine**

1136 Schematic representation of Nora virus propagation in the posterior midgut from intestinal
1137 stem cells to enterocytes. The Nora virus initially invades ISC in the midgut and remains
1138 rather quiescent. External factors such as age, infections or exposure to xenobiotics stress the
1139 host intestinal epithelium and induce ISC compensatory proliferation that ensures a degree of
1140 homeostasis by replacing damaged enterocytes. ISC cell division appears to stimulate the
1141 proliferation of the Nora virus that ultimately contaminates enterocytes. This is likely to
1142 further damage the epithelium and lead to a loss of the integrity of this intestinal barrier,
1143 allowing the enhanced passage of gut bacteria to the hemocoel.

Figure 1

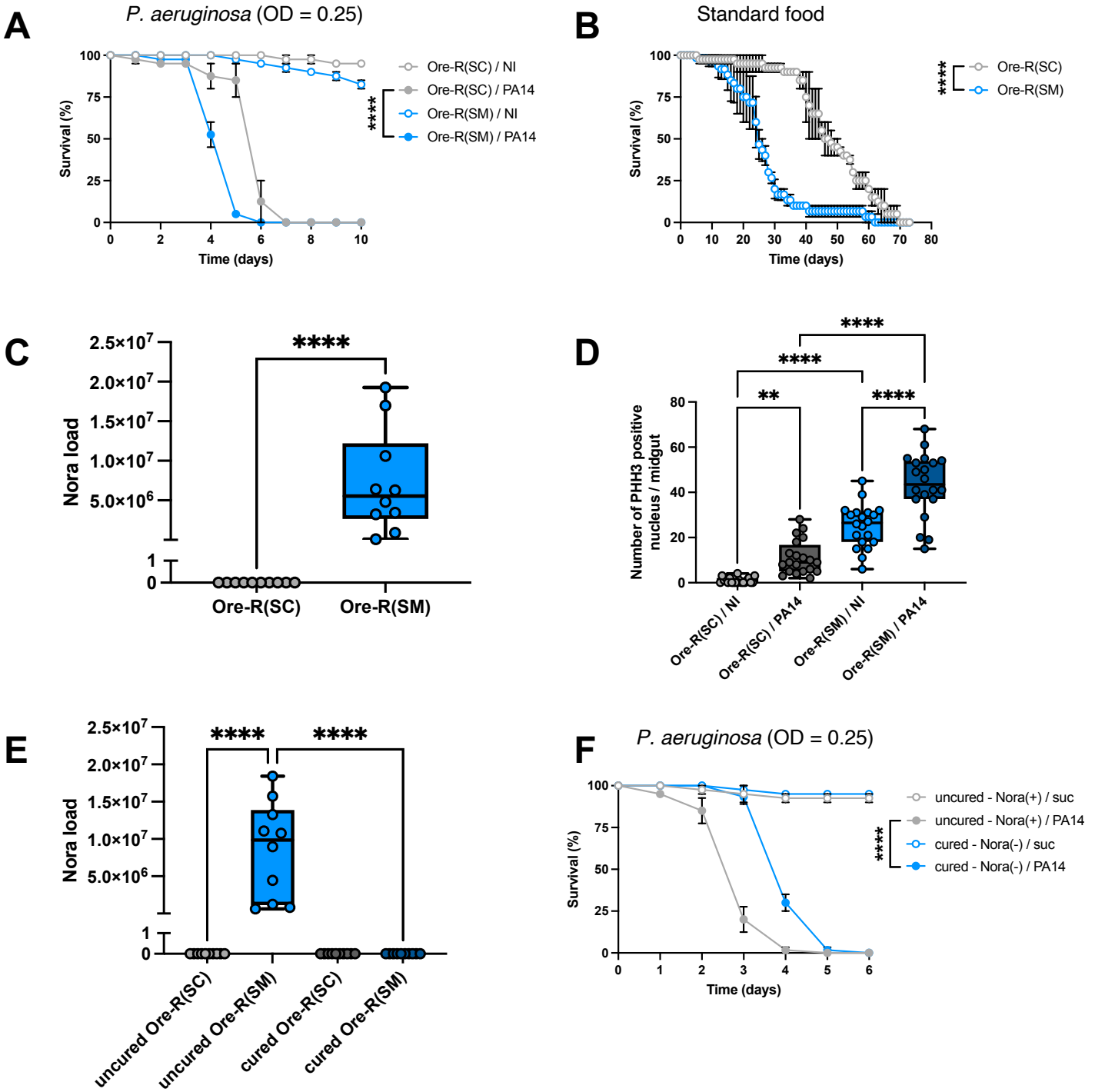
A
P. aeruginosa (OD = 0.25)
Survival (%)
Time (days)
Ore-R(SC) / NI
Ore-R(SC) / PA14
Ore-R(SM) / NI
Ore-R(SM) / PA14
****
B
Standard food
Survival (%)
Time (days)
Ore-R(SC)
Ore-R(SM)
****
C
Nora load
2.5×10^7
2.0×10^7
1.5×10^7
1.0×10^7
5.0×10^6
1
0
****
Ore-R(SC)
Ore-R(SM)
D
Number of PHH3 positive nucleus / midgut
**
****
****
****
Ore-R(SC) / NI
Ore-R(SC) / PA14
Ore-R(SM) / NI
Ore-R(SM) / PA14
E
Nora load
****
****
uncured Ore-R(SC)
uncured Ore-R(SM)
cured Ore-R(SC)
cured Ore-R(SM)
F
P. aeruginosa (OD = 0.25)
Survival (%)
Time (days)
uncured - Nora(+) / suc
uncured - Nora(+) / PA14
cured - Nora(-) / suc
cured - Nora(-) / PA14
****

Figure 2

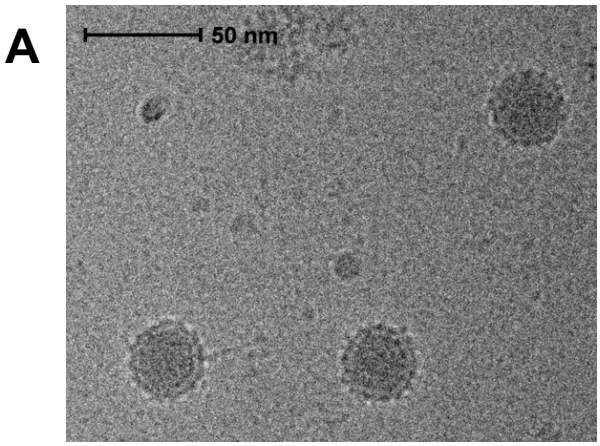
A
50 nm

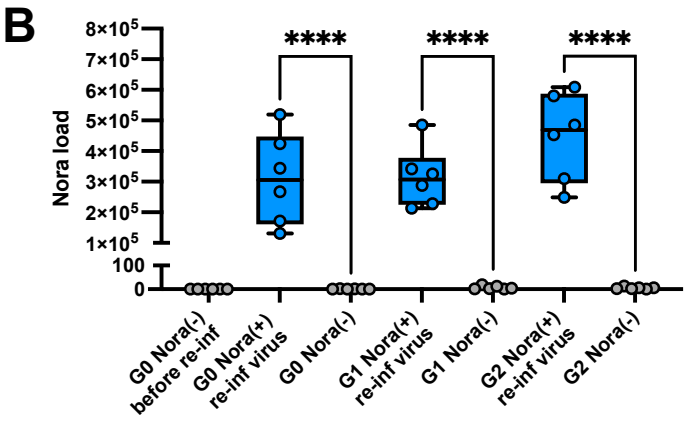
B
Nora load
8×10^5
7×10^5
6×10^5
5×10^5
4×10^5
3×10^5
2×10^5
1×10^5
100
0
****
****
****
G0 Nora(-) before re-inf
G0 Nora(+) re-inf virus
G0 Nora(-)
G1 Nora(+) re-inf virus
G1 Nora(-)
G2 Nora(+) re-inf virus
G2 Nora(-)

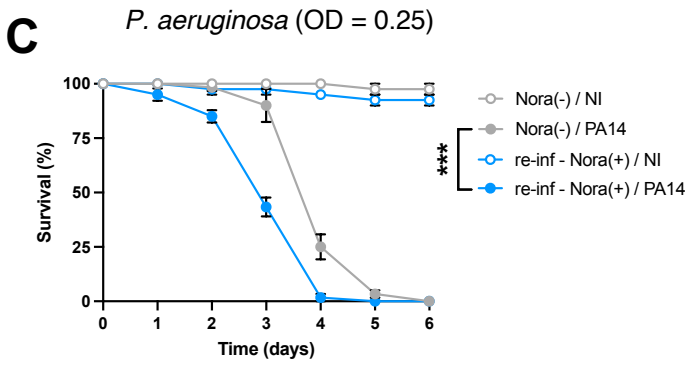
C
P. aeruginosa (OD = 0.25)
Survival (%)
Time (days)
Nora(-) / NI
Nora(-) / PA14
re-inf - Nora(+) / NI
re-inf - Nora(+) / PA14
***

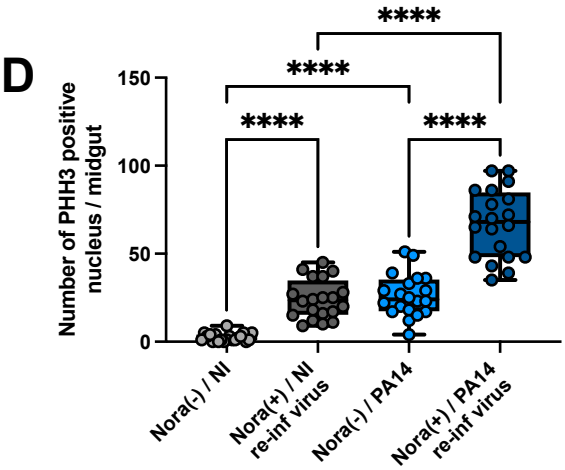
D
Number of PHH3 positive nucleus / midgut
****
****
****
****
Nora(-) / NI
Nora(+) / NI re-inf virus
Nora(-) / PA14
Nora(+) / PA14 re-inf virus

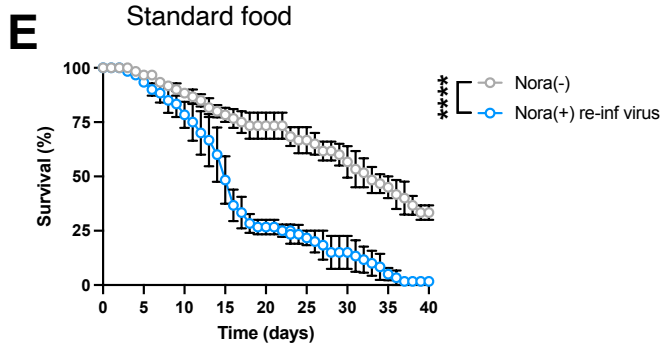
E
Standard food
Survival (%)
Time (days)
Nora(-)
Nora(+) re-inf virus
****

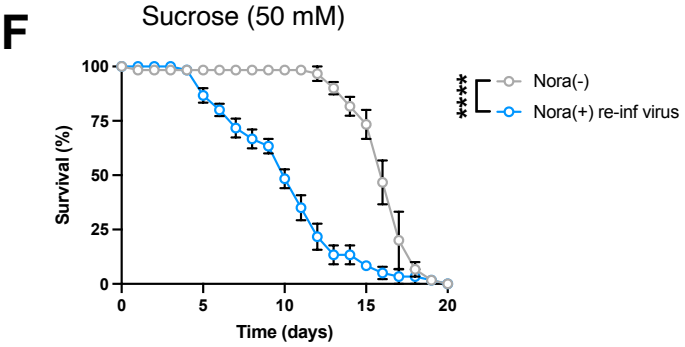
F
Sucrose (50 mM)
Survival (%)
Time (days)
Nora(-)
Nora(+) re-inf virus
****

Figure 3

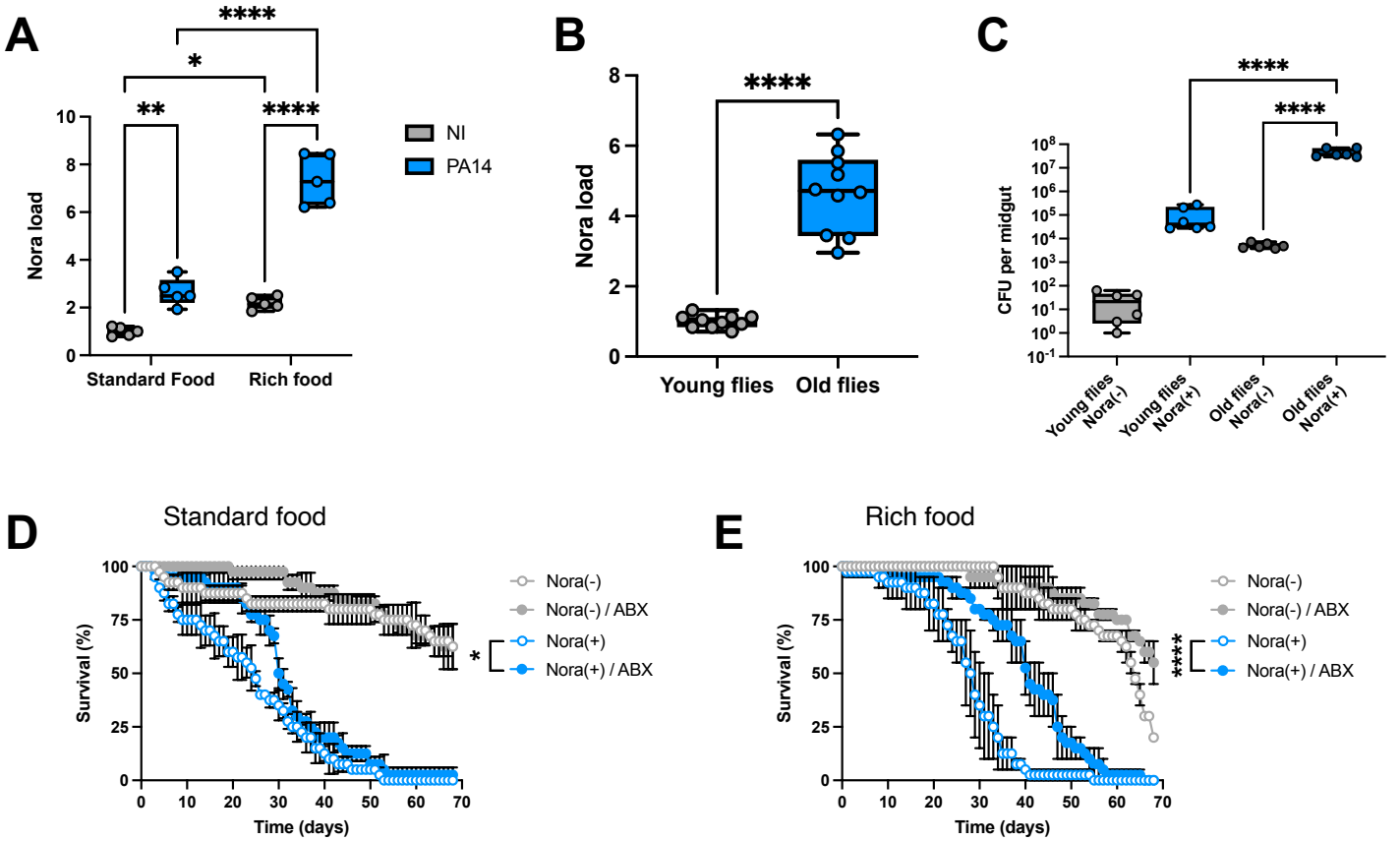
A
****
*
**
****
Nora load
NI
PA14
Standard Food
Rich food
B
****
Nora load
Young flies
Old flies
C
****
****
CFU per midgut
Young flies Nora(-)
Young flies Nora(+)
Old flies Nora(-)
Old flies Nora(+)
D
Standard food
Survival (%)
Time (days)
Nora(-)
Nora(-) / ABX
Nora(+)
Nora(+) / ABX
*
E
Rich food
Survival (%)
Time (days)
Nora(-)
Nora(-) / ABX
Nora(+)
Nora(+) / ABX
****

Figure 4

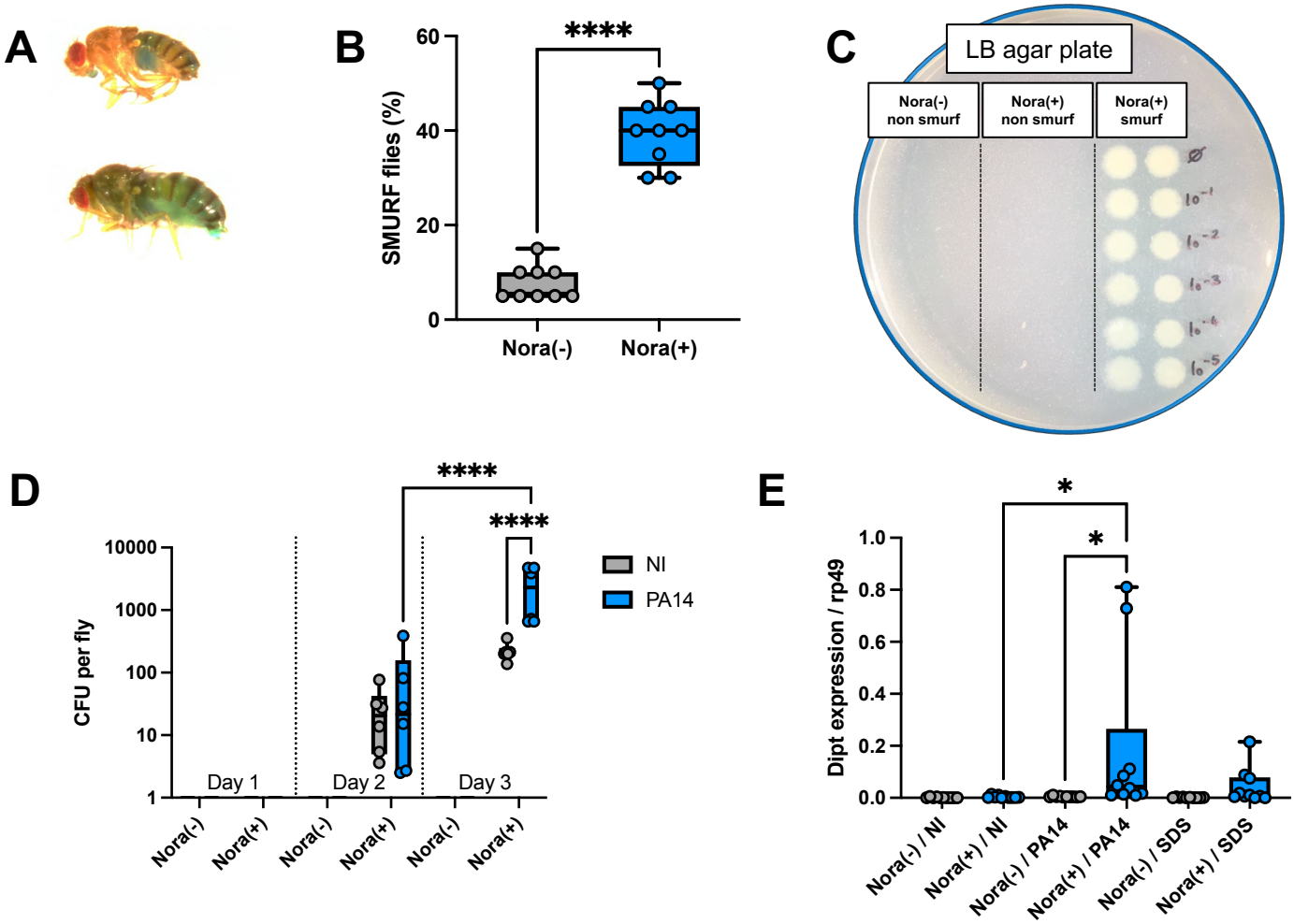
A
B
SMURF flies (%)
60
40
20
0
****
Nora(-)
Nora(+)
C
LB agar plate
Nora(-) non smurf
Nora(+) non smurf
Nora(+) smurf
D
CFU per fly
10000
1000
100
10
1
****
****
Day 1
Day 2
Day 3
Nora(-)
Nora(+)
Nora(-)
Nora(+)
Nora(-)
Nora(+)
NI
PA14
E
Dipt expression / rp49
1.0
0.8
0.6
0.4
0.2
0.0
*
*
Nora(-) / NI
Nora(+) / NI
Nora(-) / PA14
Nora(+) / PA14
Nora(-) / SDS
Nora(+) / SDS

Figure 5

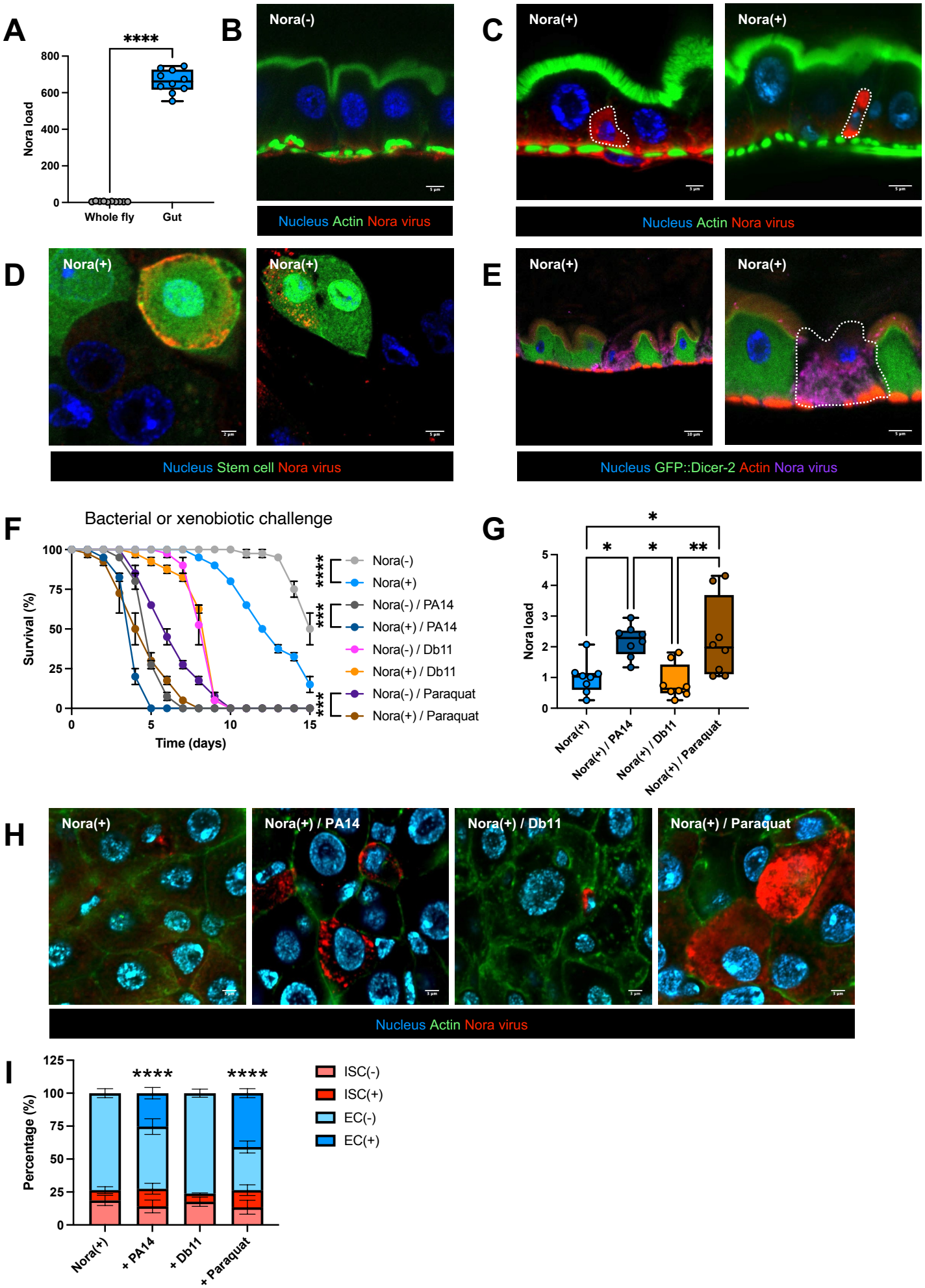
A
****
Nora load
800
600
400
200
0
Whole fly
Gut
B
Nora(-)
Nucleus Actin Nora virus
C
Nora(+)
Nora(+)
Nucleus Actin Nora virus
D
Nora(+)
Nora(+)
Nucleus Stem cell Nora virus
E
Nora(+)
Nora(+)
Nucleus GFP::Dicer-2 Actin Nora virus
F
Bacterial or xenobiotic challenge
Survival (%)
Time (days)
Nora(-)
Nora(+)
Nora(-) / PA14
Nora(+) / PA14
Nora(-) / Db11
Nora(+) / Db11
Nora(-) / Paraquat
Nora(+) / Paraquat
G
Nora load
Nora(+)
Nora(+) / PA14
Nora(+) / Db11
Nora(+) / Paraquat
H
Nora(+)
Nora(+) / PA14
Nora(+) / Db11
Nora(+) / Paraquat
Nucleus Actin Nora virus
I
Percentage (%)
ISC(-)
ISC(+)
EC(-)
EC(+)
Nora(+)
+ PA14
+ Db11
+ Paraquat

Figure 6

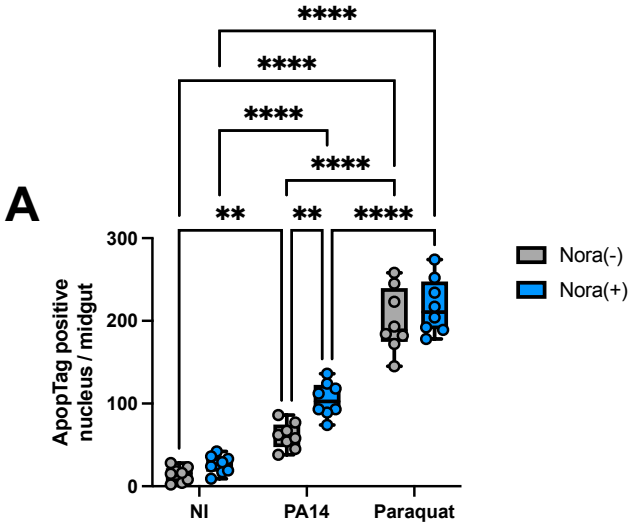
A
****
****
****
****
**
**
****
ApopTag positive nucleus / midgut
300
200
100
0
NI
PA14
Paraquat
Nora(-)
Nora(+)

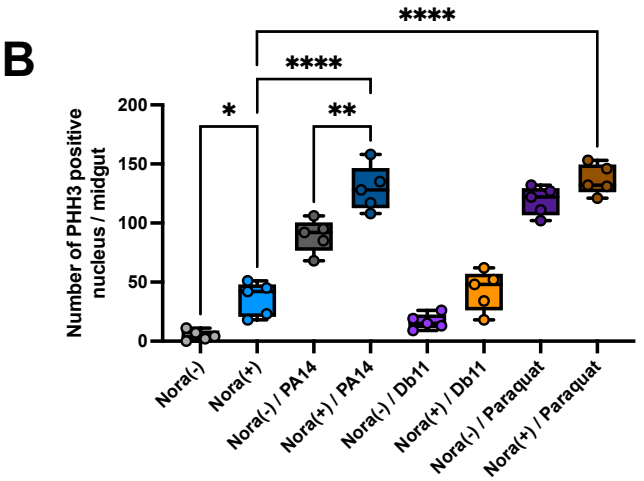
B
****
****
*
**
Number of PHH3 positive nucleus / midgut
200
150
100
50
0
Nora(-)
Nora(+)
Nora(-) / PA14
Nora(+) / PA14
Nora(-) / Db11
Nora(+) / Db11
Nora(-) / Paraquat
Nora(+) / Paraquat

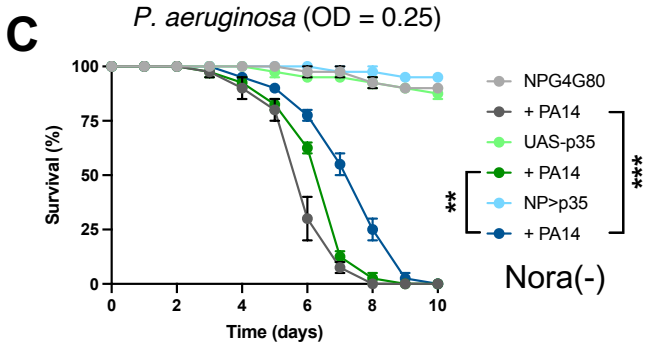
C
P. aeruginosa (OD = 0.25)
Survival (%)
100
75
50
25
0
0
2
4
6
8
10
Time (days)
NPG4G80
+ PA14
UAS-p35
+ PA14
NP>p35
+ PA14
**
***
Nora(-)

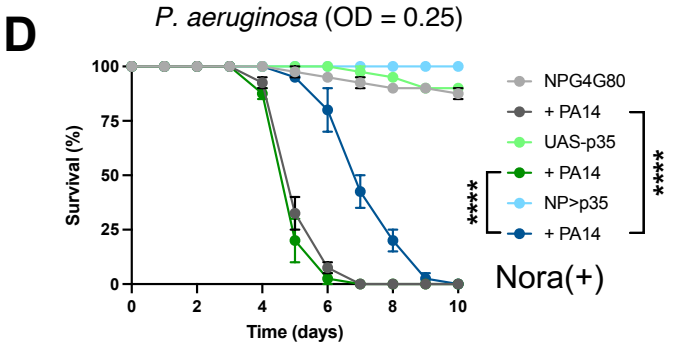
D
P. aeruginosa (OD = 0.25)
Survival (%)
100
75
50
25
0
0
2
4
6
8
10
Time (days)
NPG4G80
+ PA14
UAS-p35
+ PA14
NP>p35
+ PA14
****
****
Nora(+)

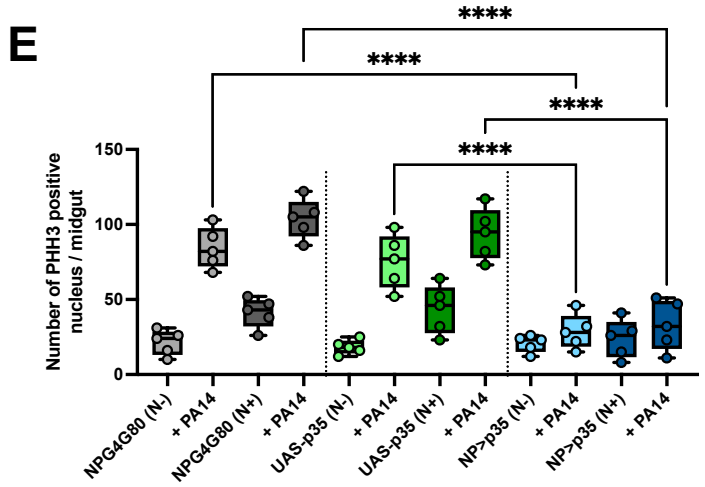
E
****
****
****
****
Number of PHH3 positive nucleus / midgut
150
100
50
0
NPG4G80 (N-)
+ PA14
NPG4G80 (N+)
+ PA14
UAS-p35 (N-)
+ PA14
UAS-p35 (N+)
+ PA14
NP>p35 (N-)
+ PA14
NP>p35 (N+)
+ PA14

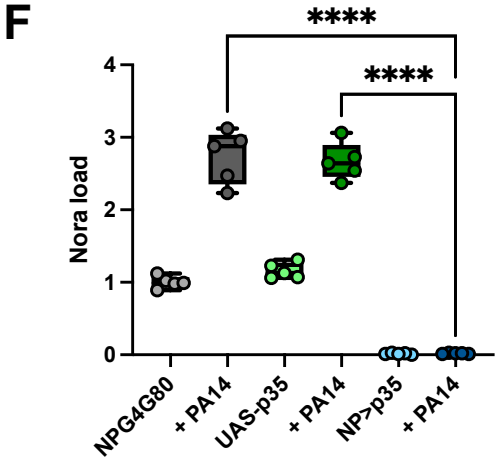
F
****
****
Nora load
4
3
2
1
0
NPG4G80
+ PA14
UAS-p35
+ PA14
NP>p35
+ PA14

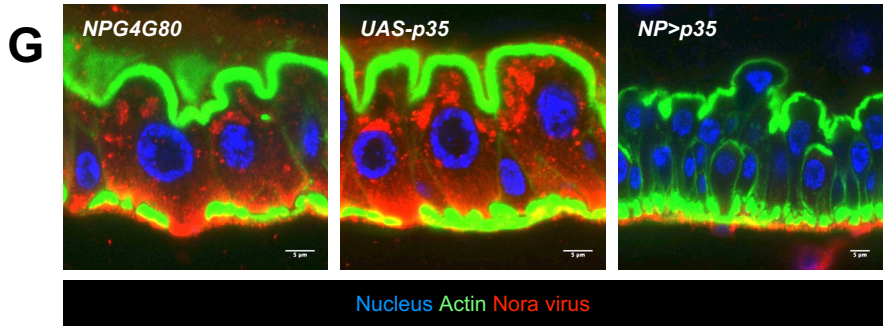
G
NPG4G80
UAS-p35
NP>p35
Nucleus Actin Nora virus

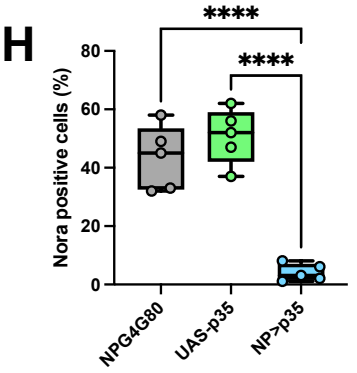
H
****
****
Nora positive cells (%)
80
60
40
20
0
NPG4G80
UAS-p35
NP>p35

Figure 7

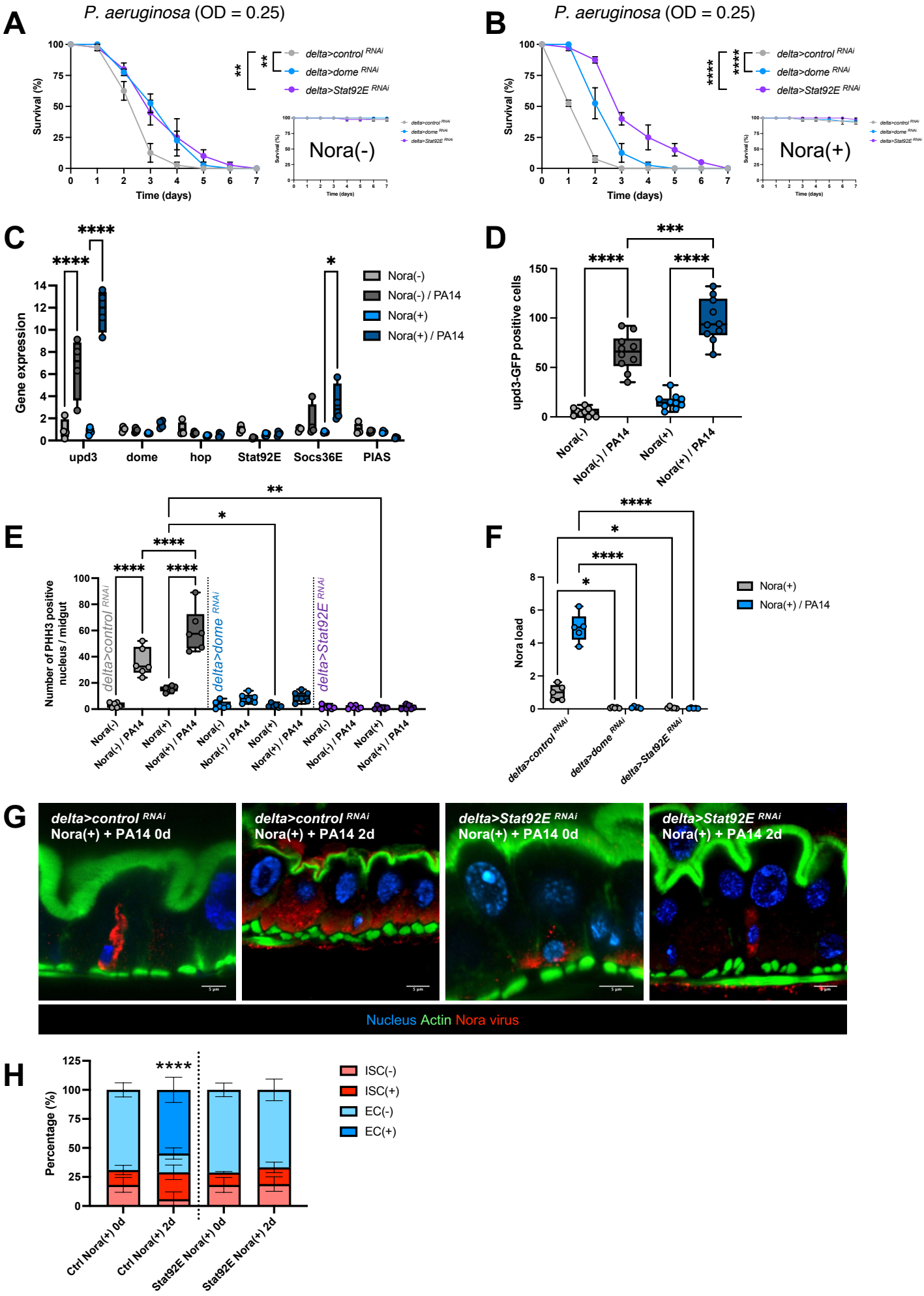
A
P. aeruginosa (OD = 0.25)
Survival (%)
Time (days)
delta>control RNAi
delta>dome RNAi
delta>Stat92E RNAi
Nora(-)
B
P. aeruginosa (OD = 0.25)
Nora(+)
C
Gene expression
Nora(-)
Nora(-) / PA14
Nora(+)
Nora(+) / PA14
upd3
dome
hop
Stat92E
Socs36E
PIAS
D
upd3-GFP positive cells
E
Number of PHH3 positive nucleus / midgut
F
Nora load
G
delta>control RNAi Nora(+) + PA14 0d
delta>control RNAi Nora(+) + PA14 2d
delta>Stat92E RNAi Nora(+) + PA14 0d
delta>Stat92E RNAi Nora(+) + PA14 2d
Nucleus Actin Nora virus
H
Percentage (%)
ISC(-)
ISC(+)
EC(-)
EC(+)
Ctrl Nora(+) 0d
Ctrl Nora(+) 2d
Stat92E Nora(+) 0d
Stat92E Nora(+) 2d

Figure 8

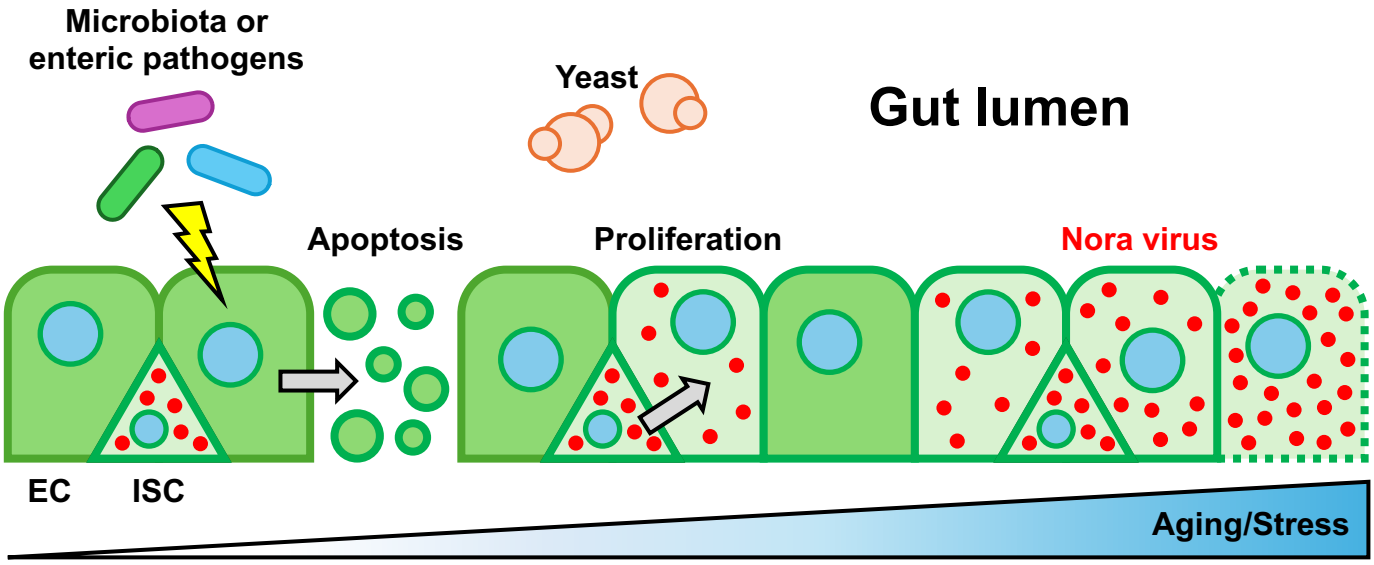
Microbiota or
enteric pathogens
Yeast
Gut lumen
Apoptosis
Proliferation
Nora virus
EC
ISC
Aging/Stress